CHARACTERIZING STATION ARIDITY AND IMPROVING THE ESTIMATES OF REFERENCE EVAPOTRANSPIRATION IN THE OKLAHOMA MESONET

By

ASEEM PAL SINGH

Bachelor of Technology in Civil Engineering
G. B. Pant University of Agriculture and Technology
Pantnagar, India
2012

Master of Technology in Environmental Management
Indian Institute of Technology
Roorkee, India
2015

Submitted to the Faculty of the
Graduate College of the
Oklahoma State University
in partial fulfillment of
the requirements for
the Degree of
DOCTOR OF PHILOSOPHY
July, 2022

CHARACTERIZING STATION ARIDITY AND IMPROVING THE ESTIMATES OF REFERENCE EVAPOTRANSPIRATION IN THE OKLAHOMA MESONET

Dissertation Approved:

Dr. Ali Mirchi

Dissertation Adviser

Dr. Saleh Taghvaeian

Dr. Sara Alian

Dr. Phillip Alderman

ACKNOWLEDGEMENTS

I would like to thank my advisor and mentor Dr. Ali Mirchi for his support and encouragement. I would also like to thank my advising committee members Dr. Saleh Taghvaeian, Dr. Sara Alian, and Dr. Phillip Alderman for their guidance and insights. Contributions from Dr. Abubakarr Mansaray and inputs and guidance from Dr. Chris Fiebrich and Mr. Wes Lee are gratefully acknowledged. I would also like to acknowledge the help and support of the faculty and staff in the Department of Biosystems and Agricultural Engineering and Oklahoma State University. This material is based upon work that is supported in part by the U.S. Department of Agriculture (USDA) Agricultural Research Service (ARS). Any opinions, findings, conclusions, or recommendations expressed in this publication are those of the author and do not necessarily reflect the view of the U.S. Department of Agriculture or the Oklahoma Mesonet. This dissertation could not be done without tremendous support of my parents- Subhash Pal Singh and Neelkamal Singh, and my sister, Shivangi.

Name: ASEEM PAL SINGH

Date of Degree: JULY, 2022

Title of Study: CHARACTERIZING STATION ARIDITY AND IMPROVING THE ESTIMATES OF REFERENCE EVAPOTRANSPIRATION IN THE OKLAHOMA MESONET

Major Field: BIOSYSTEMS ENGINEERING

Abstract: There is a consensus among the scientific community regarding the rise in air temperatures and changing precipitation patterns across the globe. Many areas around the world are expected to see increased aridity levels in the future. The trends will likely impact the agricultural water availability, especially in water-scarce regions. As freshwater water availability declines in water-scarce agricultural regions, it is important for the producers to use it efficiently. Therefore, the objectives of this dissertation are: (1) To analyze the historical trends in temperature, rainfall, and reference evapotranspiration on a climate divisional scale across Oklahoma using the available datasets to provide insights about the implications of these trends on agricultural water management; (2) To examine station aridity in the Oklahoma Mesonet stations to investigate its prevalence and spatiotemporal patterns; and (3) To demonstrate the implications of station aridity for reference evapotranspiration and improve the estimation of the reference evapotranspiration in the Oklahoma Mesonet stations to facilitate potential irrigation water savings in the State of Oklahoma. The results reveal increasing air temperature and precipitation trends on annual and seasonal scales and decreasing reference evapotranspiration trends in summer in Oklahoma which are consistent with the findings of other researchers in the Great Plains region. Station aridity is prevalent in the dry western part of the state which hinders the Mesonet's ability to provide accurate data on reference evapotranspiration. Station aridity effects are more pronounced during droughts, limiting the utility of the estimated reference evapotranspiration in areas and at times that accurate information is critically needed to support agricultural water conservation. It is demonstrated that air temperature and humidity datasets can be adjusted to improve the reference evapotranspiration estimates using the available and a newly developed methodology using NDVI.

TABLE OF CONTENTS

Chapter Page

LIST OF TABLES

Table Page

LIST OF FIGURES

Figure Page

Figure Page

CHAPTER I

INTRODUCTION

1.1. Background

There is growing consensus that climate change will affect extreme weather events, shift rainfall patterns, and increase temperatures, in turn posing risks to agricultural production worldwide (Brown et al., 2015; von Braun, 2020). The impacts of rising temperatures on increased demand for water and energy have been documented around the world (Watson et al., 1996). These effects have also been observed in the Great Plains region of the United States (U.S.) (Kukal & Irmak, 2018; Melillo et al., 2014). Increasing temperatures are altering the balance between water and energy in our ecosystems (Babst et al., 2019; Piao et al., 2014; Seager et al., 2018). Global warming is expected to intensify the global water cycle (Masson-Delmotte et al., 2021). While the extent to which a warmer future will change agroecosystems is uncertain (Seager et al., 2018), increasing temperatures will ultimately increase the evaporative demand and will substantially reduce the water storage in groundwater aquifers (Condon et al., 2020). Increased competition for limited water resources exacerbates water stress in the agricultural sector and for natural resources (Shafer et al., 2014). On one hand, increasing evaporation can increase in the intensity of storms because warmer air can hold more vapor to reach saturation. On the other hand, intensification of the hydrologic cycle can lead to increased intensity of droughts far away from storm tracks (Trenberth, 2005). Agriculture will be one of the sectors that will be highly affected

by climate change as it heavily depends on the optimum amount of precipitation, soil moisture availability, and temperature (Walthall et al., 2013). The Northern Great Plains will likely see increased precipitation while the Southern Great Plains will see longer dry periods in parts of Oklahoma (OK) and Texas (Groffman et al., 2014). As such, robust estimates of water balance will be required with the intensification of the effects of climate change (Bates et al., 2008) for efficient management of water resources. Agriculture utilizes 76% of land and contributes more than $18.2 billion to OK's economy (Shideler, 2015). Irrigation plays an important role in agricultural production, accounting for 41% of the total water use (~ 242 billion gallons), especially in the arid and semi-arid areas in western OK (Taghvaeian, 2014), which receives much less precipitation (e.g., 396 mm in the OK Panhandle) than southeastern OK with an average annual rainfall of 1286 mm.

In addition to the steep precipitation gradient, OK has a recorded history of droughts which can last from a few weeks to several years. Such droughts lead to increased water demand from surface water and groundwater resources affecting agricultural water availability. In addition to irrigated agriculture, the droughts increase competition for water among various other sectors. Therefore, it is necessary to optimize the utilization of water resources in OK and hydro-climatically similar agricultural areas where growing climate variability and change impose significant economic burden.

Evapotranspiration (ET) is the second largest component of the hydrological cycle (Gleick, 1993), which plays an important role in agricultural practices. ET represents combined loss of water through evaporation form soil surface and transpiration from plant stomata, thus, providing a basis for estimating irrigation water requirement (IWR) during their different growth stages. Numerous studies highlight the importance of changing ET patterns in different regions in the past and the future (Calanca et al., 2006; Cong et al., 2008; Gaertner et al., 2019; Rungee et al., 2019; Vadeboncoeur et al., 2018; Zhang et al., 1996). Decreasing rainfall and increasing

temperatures will increase ET (Abtew & Melesse, 2013). As such it is important for us to understand the variability in these hydro-climatological parameters because these are the key elements for effective agricultural operations. For example, accurate ET data helps improve irrigation scheduling which is the decision of when and how much of the water is to be applied to the field. Overirrigation and underirrigation both have disadvantages. Overirrigation because of overestimation of ET results in inefficient use of water, leaching of nutrients below root zone, decreased aeration, and reduced crop yields. Underirrigation as a result of underestimation of ET stresses plants and hence reduces yields (Broner, 1989).

The American Society of Civil Engineers' Standardized Penman Monteith equation (ASCE, 2005) is widely used throughout the world to estimate reference evapotranspiration (ET_{ref}). ET_{ref} is the evapotranspiration from reference surface defined as a well-watered grass surface having fixed height of 0.12 m, albedo of 0.23, and a fixed surface resistance surface resistance of 70 sm-1. Various researchers have reported overestimation in ET_{ref} estimates by over 20% in the arid stations by using the Penman Monteith method depending on the location of weather stations and the surrounding environment due to deviation of actual surface conditions from reference surface condition. Such deviations can cause inaccuracies in ET_{ref} values reported by mesoscale monitoring networks such as the OK Mesonet, which are intended to improve agricultural water management, among other things. Accurate estimation of ET_{ref} requires actively transpiring vegetation which increases the relative humidity (R.H.) of ambient air as more incoming radiation energy is consumed in the evapotranspiration process instead of heating air and soil. This results in a reduction of air temperature. Thus, monitoring stations typically record higher temperatures than what would have been observed if an actively transpiring vegetation were present leading to ET_{ref} overestimation. Many OK Mesonet stations do not meet the criteria of reference surface, a necessary condition for estimating ET_{ref}.

1.2. Objectives

This research will contribute to improved estimation of ET_{ref} in the Oklahoma Mesonet using the American Society of Civil Engineers' Standardized Penman Monteith equation (ASCE, 2005). Hence, it has the potential to facilitate water savings in the agricultural sector in OK and other regions where monitoring programs are used to inform irrigation decisions. The specific objectives of this research are:

1. To analyze the trends in temperature, rainfall, and ET_{ref} on a climate divisional scale using the available datasets from the United States Divisional Climate Dataset (USDCD) (Vose, 2014) and providing insights about the implications of these trends on agricultural water management.

2. To examine station aridity in the OK Mesonet stations to investigate its prevalence and spatiotemporal patterns. Station aridity is characterized based on deviation of actual surface conditions from reference surface condition. It is hypothesized that overestimation of ET_{ref} is more pronounced in arid regions where rainfall is not enough to meet the evapotranspiration demand of the atmosphere.

3. To demonstrate the implications of station aridity for reference evapotranspiration and improve the estimation of the reference evapotranspiration in the Oklahoma Mesonet stations to facilitate potential irrigation water savings in the State of Oklahoma.

1.3. Organization

This dissertation includes five chapters. Chapter I provides a general introduction of the dissertation and explains, in brief, the objectives of this research. Chapter II looks at the historical trends in hydroclimatic variables including air temperature, precipitation, and ET_{ref} by utilizing historical datasets for the 70-year period from 1951 to 2021. Chapter III characterizes station aridity in the Oklahoma Mesonet stations which causes the overestimation of ET_{ref}.

Spatiotemporal characteristics of the station aridity are discussed which provides a better understanding of the limitations of weather monitoring networks in estimating ET_{ref}. Chapter IV investigates and improves the overestimation of ET_{ref} in the Oklahoma Mesonet stations. Chapter V summarizes the conclusions and suggests future work.

CHAPTER II

ANALYSIS OF CLIMATIC TRENDS IN CLIMATE DIVISIONS OF OKLAHOMA, U.S.

2.1. Introduction

Rising greenhouse gas emissions continue to worsen the impacts of climate change on humans and ecosystems (Kumar et al. 2012; Masson-Delmotte et al. 2021; Mastrandrea et al. 2011; Solomon et al. 2007). As a result, increasing global temperatures and precipitation changes have become a focal point of climate change research (Jain and Kumar 2012; Martínez et al. 2010; Myhre et al. 2019; Papalexiou and Montanari 2019). Increased number of dry periods and increasing intensity of precipitation (extreme rainfalls occurring over shorter spans) can affect surface water availability and evapotranspiration, which have important implications for agricultural water management. Analysis of long-term climate records facilitates identifying priority areas for agricultural water resources planning and adaptive management (Anwar et al. 2013; Chauhan et al. 2014; Piao et al. 2010).

In the past few decades, researchers have analyzed temperature, precipitation, and reference evapotranspiration (ET_o) trends worldwide at national, regional, and local scales (Benestad 2013; Gobiet et al. 2014; Huntington 2006; Jain and Kumar 2012; Twardosz et al. 2021). Easterling et al. (1997) showed that increasing temperatures in most parts of the globe are partly due to narrower mean diurnal temperature ranges. Capparelli et al. (2013) reported statistically significant cooling trends in the southeastern and warming trends in the rest of the contiguous U.S. Pathak et al. (2017) observed increasing spring temperature trends, increasing minimum

temperature and precipitation trends, and decreasing ET_o trends in the mid-western U.S. Predominantly increasing minimum temperature, precipitation, and decreasing ET_o trends have been reported in majority of the counties in the U.S. Great Plains (Kukal and Irmak 2016 a,b). These findings are consistent with observed increased mean maximum and minimum temperatures in Nebraska, U.S. (Dos Santos et al. 2022)

Oklahoma is a part of the Southern Great Plains region of the U.S. where temperature has been projected to increase by 2.0-2.8°C by the mid-21st century and by 2.4-4.7°C by the late 21st century. Projections have also indicated increase in the frequency and intensity of severe storms in the region (Bartush et al. 2018). The presence of a marked shift between the humid eastern U.S. and the arid western regions between the 97^{th} and 99^{th} meridians (Seager et al. 2018; Webb 1931) has created diverse climate divisions in Oklahoma. Over the past century, the state has been impacted by severe droughts with substantial variability and at decadal time scales (Tian and Quiring 2019). There have also been record-breaking precipitation events that led to severe floods across the state (Jennrich et al. 2020). A continued decrease in open surface water body area was reported in Oklahoma from 1984 to 2015, likely in direct response to precipitation patterns and an inverse relationship with temperature (Zou et al. 2017).

This objective of this paper is to document the historical climatic trends (from 1951 to 2021) in Oklahoma, U.S. in terms of changes in precipitation, air temperature, and ET_o in the state's nine climate divisions. We used a suite of tests to provide a robust characterization of the annual and seasonal trends in climatological time series for Oklahoma from the National Oceanic and Atmospheric Administration (NOAA) Monthly U.S. Climate Divisional Database. We applied widely used non-parametric tests, including the Modified Mann-Kendall (MMK) (Hamed and Rao 1998; Kendall 1975; Mann 1945) and the Sen's slope (SNS) estimator (Gilbert 1987; Sen 1968) to identify significant ($p < 0.05$) positive and negative trends. Further, we applied a new approach known as the Innovative Trend Analysis (Şen 2012; Şen 2017), and least square

regression tests (Haan 1977) to confirm and support the results of the non-parametric tests. The research informs agricultural production and natural resource management based on an improved understanding of the gradual climatic changes across the state through time using a statistical lens.

2.2. Materials and Methods

2.2.1. Study Area

The state of Oklahoma is situated roughly from 33°37’ N to 37° N latitudes and 94°26’ W to 103° W longitudes in south central U.S. It has an area of 181,048 km^2, sloping from the high plains in the western Panhandle, with the highest elevation being 1,516 m above mean sea level (amsl), to the wetlands in the southeastern part of the state with 88 m amsl at its lowest elevation. The terrain is nearly flat in the western Panhandle to rolling mountains in central Oklahoma. Mountains include the Ouachita Mountains in the southeast and Ozark plateau with forests in its northeastern part (Arndt 2003). Its climate ranges from semi-arid in the west to humid subtropical in the east based on Köppen climate classification (Oklahoma Climatological Survey 2020). The state is divided into nine climate divisions (Fig. 1) that are climatologically uniform (Guttman and Quayle 1996; Karl and Riebsame 1984).

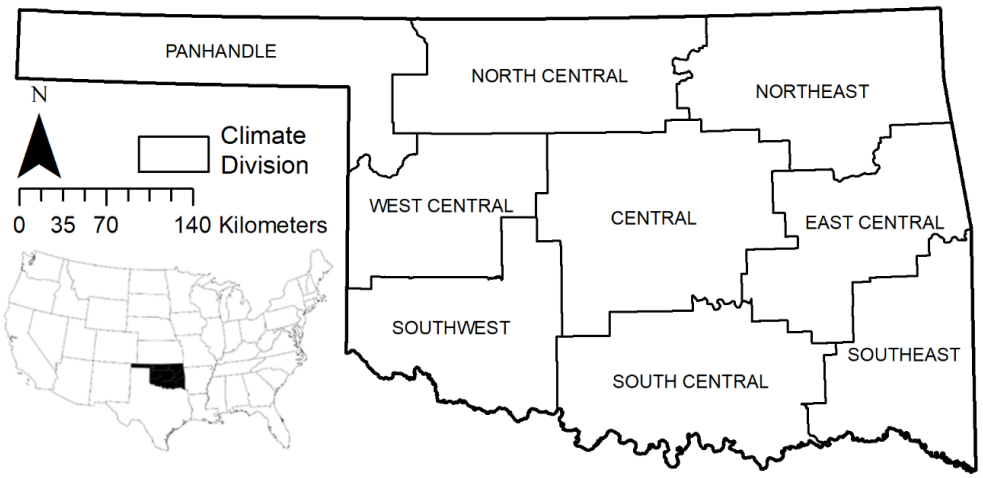

Fig. 1 Map of Oklahoma and its nine climate divisions.

2.2.2 Data

Seventy years of data (from 1951 to 2021) were obtained from the NOAA Monthly U.S. Climate Divisional Database (hereafter, climate divisional data), including mean monthly maximum, average, and minimum air temperature (T_{max}, T_{avg} and, T_{min}, respectively), and precipitation (P). The climate divisional data are provided by the Global Historical Climatology Network – daily (GHCN –Daily) (Menne et al. 2012) dataset, which contains stations from various major climate networks including Cooperative Observer program (COOP), Automated Surface Observing System (ASOS), National Interagency Fire Center (NIFC), Remote Automatic Weather Station (RAWS), USDA Snow Telemetry (SNOTEL), Environment Canada (EC) network, and Servicio Meteorologico Nacional (SMN) from Mexico. The data are constructed using climatologically aided interpolation (CAI), which addresses network and topographic variability (Vose et al. 2014; Willmott and Robeson 1995). The data were grouped into averages representing winter (December, January, and February), spring (March, April, and May), summer (June, July and, August), and fall (September, October, and November). Further, the 12-month SPI were also used to characterize historical droughts in the climate divisions based on drought categories of the U.S. drought monitor. The meteorological drought categories include abnormally dry (D0; SPI: -0.5 to

-0.7), moderate (D1; SPI: -0.8 to -1.2), severe (D2; SPI: -0.8 to -1.2), extreme (D3; SPI: -1.6 to -1.9), and exceptional (D4; SPI: -2.0 or less).

2.2.3 Data analysis

1. The Modified Mann-Kendall and Sen's slope tests

The MMK (Hamed and Rao 1998; Kendall 1975; Mann 1945) and the SNS estimator, also known as the Theil-Sen test (Gilbert 1987; Sen 1968), have been extensively used in trend analysis studies for various climatological variables. The MMK is a test used to determine whether there is a monotonic upward or downward trend in a time series. The test does not require the data to be normally distributed. The null hypothesis (H_o) is that there is no trend in the data and the alternative hypothesis (H_a) is that a trend exists. The MMK test accounts for lag-1 autocorrelation in the time series and it is independent of the distribution of the dataset (Hurrell 2017). The S statistic for this test is calculated by Eq.1.

$$S = \sum_{i=1}^{n-1} \sum_{j=i+1}^{n} sign(x_j - x_i) \qquad \textit{Eq. 1}$$

where $sign(x_j - x_i)$ is equal to +1, 0, or -1. The variance associated with S is calculated as shown in Eq. 2.

$$var(S) = \frac{n(n-1)(2n+5) - \sum_{k=1}^{m} t_k(t_k-1)(2t_k+5)}{18} \qquad \text{Eq.2}$$

where m is the number of tied zero difference groups and $t_k$is the number of tied data points in the k^{th}group. The standardized test statistic Z is calculated as shown in Eq. 3.

$$Z = \begin{cases} \dfrac{S-1}{\sqrt{var(S)}}, if\ S > 0 \\ 0, \quad if\ S = 0 \\ \dfrac{S+1}{\sqrt{var(S)}}, if\ S < 0 \end{cases} \qquad \text{Eq.3}$$

Positive values of Z indicate increasing trend while negative values indicate decreasing trend. Trends are significant if $|Z| > Z_{1-\alpha/2}$ for the desired value of significance, i.e., $p < 0.05$) denoting 95% confidence level for testing the null hypothesis. The test was performed using "mmkh" function from the "modifiedmk" (version 1.6) package (Patakamuri and O'Brien 2021) in R-Studio.

The Sen's slope test is used to quantify significant linear trends in a time series. It provides additional information about a statistically significant trend (as detected by the MMK) by estimating the quantity per time by which the trend occurs. The SNS is insensitive to extreme values in the dataset and hence is considered more robust than a linear regression method. The slope T_i is given by Eq. 4.

$$T_i = \frac{x_j - x_k}{j - k}, \qquad j > k \qquad \text{Eq.4}$$

where x_j and x_k are the parameter values at time j and k, respectively. The median of these values is calculated as follows:

$$\beta = \begin{cases} T_{\frac{n+1}{2}}, & n\ is\ odd \\ \dfrac{1}{2}\left(T_{\frac{n}{2}} + T_{\frac{n+2}{2}}\right), & n\ is\ even \end{cases} \qquad \text{Eq.1}$$

where positive value of β indicates an increasing trend while negative value indicates decreasing trend.

2. The Innovative trend analysis (ITA)

The ITA is a new approach that has recently been introduced to indicate the possibilities of floods and droughts (Dabanlı et al. 2016). It helps to determine if a phenomenon is changing or remains stable with time. The ITA is free from the assumptions of normality and serial autocorrelation. The time series data was divided into two equal halves one of which was placed on the X-axis and the other, the Y-axis. Increasing and decreasing trends were determined based on the position of the paired data relative to a 1:1 reference line. When the data was in the upper half of the 1:1 line, it indicated an increasing trend, and the lower half of the 1:1 line indicated a decreasing trend. The slope of the ITA test may also be used to indicate an increasing or decreasing trend. The "innovtrend" function from the "trendchange" (version 1.1) R package was used (Patakamuri and Das 2019) to carry out the ITA test.

3. Least Squares Regression (LSR)

The simple Least Square Regression (LSR) method is used to plot a line of best fit across the least square of residuals in the time series of a parameter of concern, assuming the data have normally distributed residuals (Kleinbaum et al. 2013). The line of best fit is drawn such that the sum of square of the data points (i.e., X: independent variable (year) and Y: dependent variable (climate variable)) from the line is minimum. A positive slope indicates an increasing trend and vice versa. The slope (m) and intercept (b) of the line of best fit are given by Equations 6 and 7.

$$m = \frac{n(\sum xy) - (\sum x \sum y)}{n(\sum x^2) - (\sum x)^2} \qquad \textit{Eq. 1}$$

$$b = \frac{(\sum x^2)(\sum y) - (\sum x)(\sum xy)}{n(\sum x^2) - (\sum x)^2} \qquad \textit{Eq. 2}$$

4. Hargreaves-Samani method to calculate ETo

The Hargreaves-Samani equation (Hargreaves and Samani 1985) is widely applied to estimate ET_o. We used input data from the mean values of T_{max}, T_{min}, and extraterrestrial solar radiation, which can be estimated from the latitude and day of the year. The calibrated equation is given by Equation 8.

$$ET_o = 0.0023 \times R_A \times (T_{max} - T_{min})^{0.5} \times (T_{avg} + 17.8) \qquad Eq.\ 8$$

where, ET_o= Short grass reference evapotranspiration and R_A = extraterrestrial solar radiation.

2.3. RESULTS AND DISCUSSION

2.3.1 Overview of the climate variables

The mean annual T_{max}, T_{avg}, T_{min}, P, and ET_o are summarized in Table 1 to provide an overview of the climatic variables in the nine climate divisions of Oklahoma. The southern climate divisions had the highest T_{max} and T_{avg} followed by the central, and then the north, indicating a northward decreasing temperature gradient across the state (Fig 2). Minimum temperature gradients followed a diagonal trend from the northwest (the coldest) to the southeast (the warmest) (Fig 2). Overall, annual mean temperatures do not vary greatly across the climate divisions; mean T_{max} ranged from 21.29 °C to 23.28 °C, mean T_{avg} ranged from 13.66 °C to 16.80 °C, and mean T_{min} ranged from 7.75 °C to 10.32 °C (Table 1).

The precipitation gradient trended from west (the minimum) to east (the most) (Fig 2). The highest precipitation was recorded in the southeast with a mean annual value of 1,258 mm, and the lowest was recorded in the Panhandle with a mean annual precipitation of 499 mm. The eastern climate divisions receive southerly winds which bring in moisture from the Gulf of Mexico while the western part is dry receiving significantly less precipitation (Illston et al. 2004; Liyan Tian et al. 2019). The ET_o ranged from 1,261 mm in the Northeast to 1,390 mm in the

Panhandle and did not show a clearly defined spatial trend across the nine climate divisions (Fig 2).

The relatively small coefficients of variation (CV) and corresponding small ranges of CV for temperature (CV: 5.7-9.3%) and ET_o (CV: 3.2-3.8%) reflect minimal variation of these variables (Table 1). By contrast, variation in precipitation is comparatively larger than in temperature in all climate divisions with CVs ranging between 19.1% and 22.5%. Such variability in P makes Oklahoma's agricultural sector vulnerable to water scarcity, especially in the western half of the state where the majority of the irrigated areas are located (Taghvaeian et al. 2015).

Table 2.1. Annual mean and coefficient of variation (CV) of temperature (°C), precipitation (mm), and reference evapotranspiration (mm) for the nine climate divisions of Oklahoma

Climate Division	T_{max}		T_{avg}		T_{min}		P		ET_o	
	Mean	CV	Mean	CV	Mean	CV	Mean	CV	Mean	CV
Panhandle	21.4	0.040	13.7	0.048	5.9	0.093	499	0.191	1347	0.032
North Central	21.6	0.044	14.7	0.052	7.8	0.089	752	0.219	1322	0.037
Northeast	21.3	0.041	15.0	0.047	8.7	0.073	1025	0.207	1261	0.038
West Central	22.1	0.042	15.1	0.048	8.2	0.075	678	0.222	1349	0.038
Central	22.2	0.040	15.7	0.045	9.2	0.070	898	0.203	1319	0.037
East Central	22.2	0.038	15.9	0.042	9.6	0.063	1124	0.208	1300	0.037
Southwest	23.2	0.039	16.3	0.043	9.5	0.067	718	0.219	1390	0.037
South Central	23.3	0.035	16.8	0.038	10.3	0.057	983	0.225	1363	0.038
Southeast	22.6	0.036	16.1	0.042	9.7	0.069	1258	0.203	1331	0.038

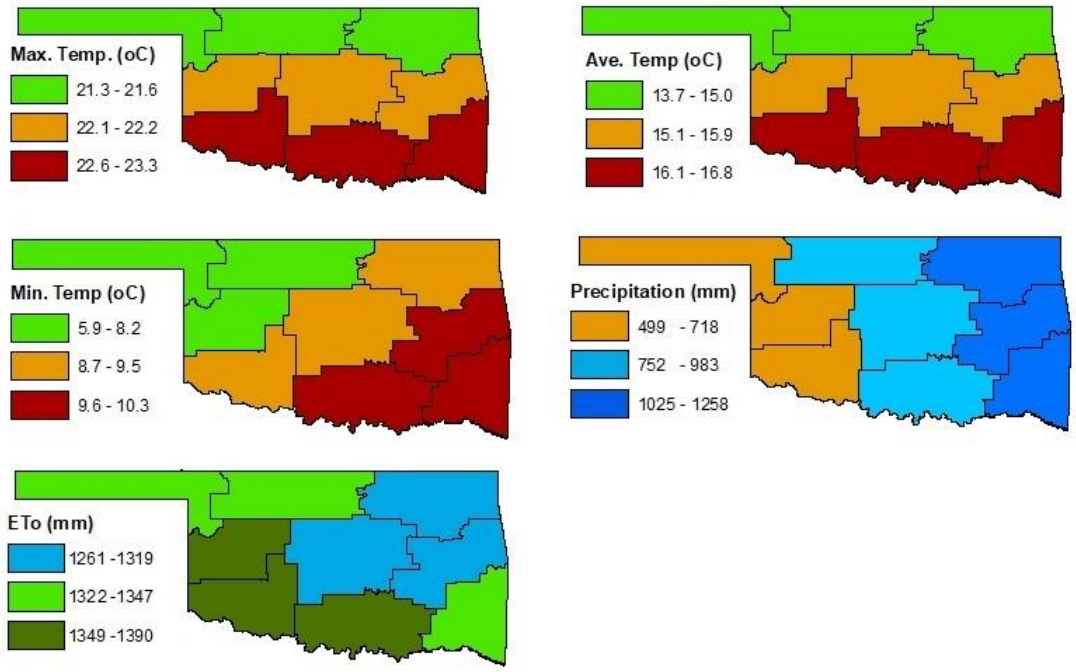

Fig. 2.2. Spatial gradients of climate variables across the climate divisions. ET_o denotes potential evapotranspiration of reference crop (i.e., dense, well-watered, stress-free grass or alfalfa having a specified height, surface resistance, and albedo).

2.3.2 Spatiotemporal trends in climatic variables

1. Temperature trends

Temperature showed a generally increasing annual trend across the state (Fig. 3). However, annual increase in T_{max} from 1951 to 2021 was not statistically significant based on the MMK test at the 95% confidence level ($p < 0.05$). The annual increase in T_{min}, on the other hand, was significant in all the climate divisions. Annual increase in T_{avg} was significant in the predominantly agricultural western climate divisions. Seasonally, most statistically significant increasing trends were observed in T_{avg} and T_{min} while the increases in T_{max} were not statistically significant. Increasing trends in T_{max}, $T_{avg,}$ and T_{min} were observed in spring, fall, and winter across the state. The increase in spring T_{min} was statistically significant in all the climate divisions except the Panhandle and South Central. Likewise, T_{min} showed a statistically significant increasing trend in some climate divisions in summer (North Central and Southeast), fall

(Northeast, Southeast, and Southwest), and winter (North Central and Southwest). The summer season had decreasing T_{max} and T_{avg} trends in Northeast, East Central, Central, and South-Central climate divisions. Only the West Central and Panhandle divisions showed increasing summer T_{max} trends, albeit statistically insignificant.

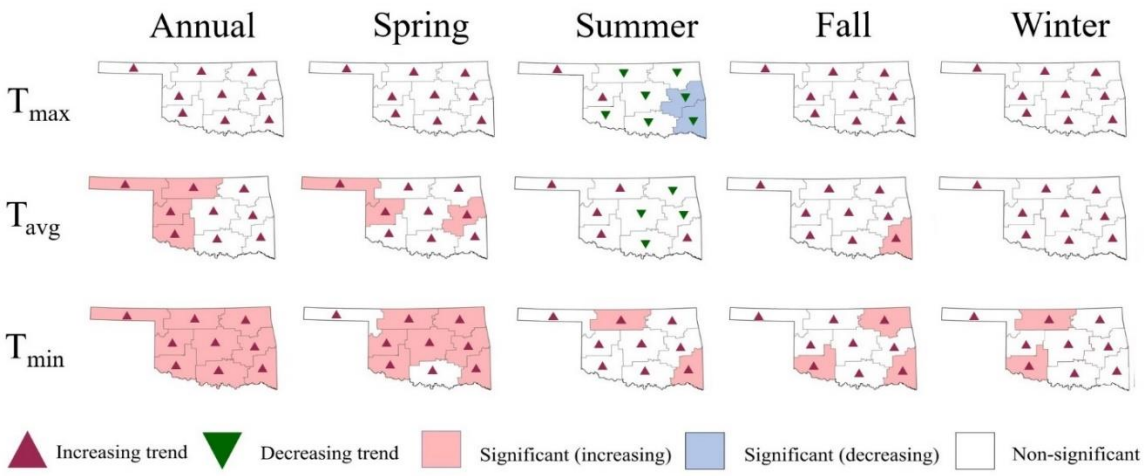

Fig. 2.3. Annual and seasonal trends in T_{max}, T_{avg}, and T_{min} based on the MMK test. The shaded divisions represent statistical significance at the 95% confidence level ($p < 0.05$).

Statistical significance of annual and seasonal temperature trends and their magnitudes are presented in Table 2. The magnitude of increase in T_{max} on annual time scale ranges from a minimum of 0.005 °C/yr ($p = 0.10$) in the Southeast to a maximum of 0.012 °C/yr ($p = 0.06$) in the Panhandle and West Central climate divisions. Although these increases are statistically insignificant at 95% confidence level, it is notable that the western parts of the state (Panhandle, West Central, and Southwest) have greater magnitudes of T_{max} slope compared to the eastern parts (Northeast, East Central, and Southeast) with slopes <0.006 °C/yr. In the spring and fall seasons, respectively, western parts of the state had the greatest magnitude of slope (0.013 °C/yr and 0.012 °C/yr), followed by the central (0.007 °C/yr and 0.008 °C/yr) and eastern parts (0.006

°C/yr and 0.007 °C/yr). A similar west-to-east decreasing gradient in the magnitude of slopes was not found for the summer and winter seasons.

The Panhandle and West Central climate divisions showed statistically significant increasing T_{avg} trends with slopes, respectively, equaling 0.010 °C/yr ($p = 0.03$) and 0.012 °C/yr ($p = 0.02$) annually, and reaching as high as 0.015 °C/yr ($p = 0.04$) and 0.020 °C/yr ($p = 0.05$) for the spring season. North Central and Southwest divisions, too, had significant T_{avg} increases of 0.010°C/yr ($p < 0.02$) or more. Like T_{max}, the magnitude of slopes for T_{avg} follows a west-to-east pattern in the spring and fall seasons; the western parts of the state showed the greatest average slope followed by the central and eastern parts. In summer, the magnitude of slopes for T_{avg} were generally small (-0.001-0.006°C/yr). Larger T_{avg} slopes were observed in central and eastern parts (0.013°C/yr) compared to the western part (0.010°C/yr) for winter.

Increasing T_{min} trends were observed throughout the state in both annual and seasonal timescales. Statistically significant positive trends were found for annual T_{min} in the Southeast (0.016°C/yr, $p = 0.00$) followed by North Central (0.014°C/yr, $p = 0.00$), Southwest (0.013°C/yr, $p = 0.00$), and the rest of the climate divisions (0.009-0.011 °C/yr, $0.00 \leq p \leq 0.01$). Most of the climate divisions show statistically significant increasing T_{min} trends in the spring season when greater slopes were observed in the agriculturally productive West Central and Southwest (0.014°C/yr) compared to the eastern climate divisions (0.008-0.012 °C/yr). In the summer season, a south-north pattern was observed in the magnitude of average slopes of T_{min}; Southwest, South Central, and Southeast had an average slope of 0.015 °C/yr followed by West Central, Central, and East Central (0.007 °C/yr) and Panhandle, North Central, and Northeast (0.005 °C/yr). This pattern largely holds in the fall season. The increase in winter T_{min} was statistically significant in the North Central (0.015°C/yr) and the Southwest (0.012°C/yr) divisions.

Table 2.2. Annual and seasonal Modified Mann-Kendall and Sen's slope tests for temperatures

Climate Division	Time Scale	T_{max}		T_{avg}		T_{min}	
		MMK (Z)	SNS (°C/yr)	MMK (Z)	SNS (°C/yr)	MMK (Z)	SNS (°C/yr)
Panhandle	Annual	1.629	0.012	**2.058***	**0.010**	**2.393**	**0.009**
	Spring	1.687	0.016	**2.015**	**0.015**	1.886	0.009
	Summer	0.129	0.001	0.228	0.001	0.113	0.000
	Fall	1.032	0.011	1.320	0.009	1.380	0.008
	Winter	0.366	0.002	0.883	0.006	1.494	0.010
North Central	Annual	1.526	0.009	**2.260**	**0.012**	**3.019**	**0.014**
	Spring	0.997	0.011	1.851	0.014	**2.556**	**0.016**
	Summer	-0.774	-0.006	0.181	0.001	**2.168**	**0.008**
	Fall	1.042	0.011	1.725	0.011	**1.976**	**0.013**
	Winter	1.052	0.012	1.943	0.014	**2.099**	**0.015**
Northeast	Annual	0.732	0.005	1.660	0.008	**4.754**	**0.011**
	Spring	1.191	0.009	1.742	0.011	**2.148**	**0.011**
	Summer	-1.439	-0.010	-0.238	-0.001	1.725	0.006
	Fall	0.132	0.001	1.210	0.005	1.603	0.010
	Winter	1.022	0.009	1.484	0.011	1.514	0.013
West Central	Annual	1.876	0.012	**2.289**	**0.012**	**2.489**	**0.011**
	Spring	1.538	0.014	**1.926**	**0.020**	**2.194**	**0.014**
	Summer	0.044	0.000	0.327	0.002	1.117	0.005
	Fall	1.389	0.014	1.757	0.011	1.551	0.010
	Winter	0.908	0.010	1.360	0.011	1.608	0.013
Central	Annual	1.583	0.008	1.954	0.010	**2.497**	**0.011**
	Spring	1.429	0.014	1.846	0.020	**2.541**	**0.011**
	Summer	-1.076	-0.006	-0.165	0.000	1.701	0.006
	Fall	1.298	0.009	1.769	0.010	1.601	0.010
	Winter	1.399	0.013	1.880	0.015	1.821	0.015
East Central	Annual	1.026	0.006	1.651	0.008	**2.425**	**0.010**
	Spring	1.539	0.009	**2.204**	**0.010**	**3.358**	**0.008**
	Summer	**-3.241**	**-0.006**	-0.173	-0.001	0.720	0.004
	Fall	0.630	0.005	1.834	0.008	1.802	0.010
	Winter	1.196	0.011	1.523	0.012	1.385	0.012
Southwest	Annual	1.702	0.010	**3.227**	**0.012**	**3.301**	**0.013**
	Spring	10.97	0.010	1.677	0.012	**3.105**	**0.014**
	Summer	-0.099	-0.000	0.680	0.004	1.831	0.009
	Fall	1.345	0.011	1.823	0.013	**2.117**	**0.013**
	Winter	0.799	0.008	1.786	0.014	**1.424**	**0.012**
South Central	Annual	0.039	0.000	1.009	0.005	**2.488**	**0.010**
	Spring	0.114	0.000	1.067	0.006	1.856	0.018
	Summer	-1.859	-0.011	-0.208	-0.001	1.490	0.008
	Fall	0.258	0.003	0.931	0.004	1.194	0.008
	Winter	0.048	0.004	1.141	0.009	1.424	0.012
Southeast	Annual	0.904	0.005	1.836	0.010	**3.677**	**0.016**
	Spring	1.027	0.005	1.941	0.010	**2.144**	**0.012**
	Summer	-0.59	-0.004	1.121	0.006	**2.581**	**0.017**
	Fall	0.898	0.007	**2.142**	**0.012**	**2.884**	**0.019**
	Winter	0.913	0.007	1.692	0.014	1.945	0.014

* Bold values indicate statistical significance at 95% confidence level for the Mann-Kendall test.

The results of the ITA and simple LSR for T_{max}, $T_{avg,}$ and T_{min} show significant warming trends, supporting the results of the MMK and SNS tests. For example, summers in North Central and

Southeast, which had a statistically significant decline in T_{max} based on the MMK and SNS, show decreasing trends with majority of points lying below the no trend (1:1) line in the ITA test (Fig 4). For increasing trends, most of the points lie above (1:1) line as shown for spring T_{min} for West Central and Southwest, and T_{avg} for Panhandle and West Central divisions (Fig 4). Similarly, the statistically significant increasing trends of annual T_{avg} and T_{min} are confirmed by the positive slopes from LSR for the Panhandle and Southwest climate divisions (Fig 5).

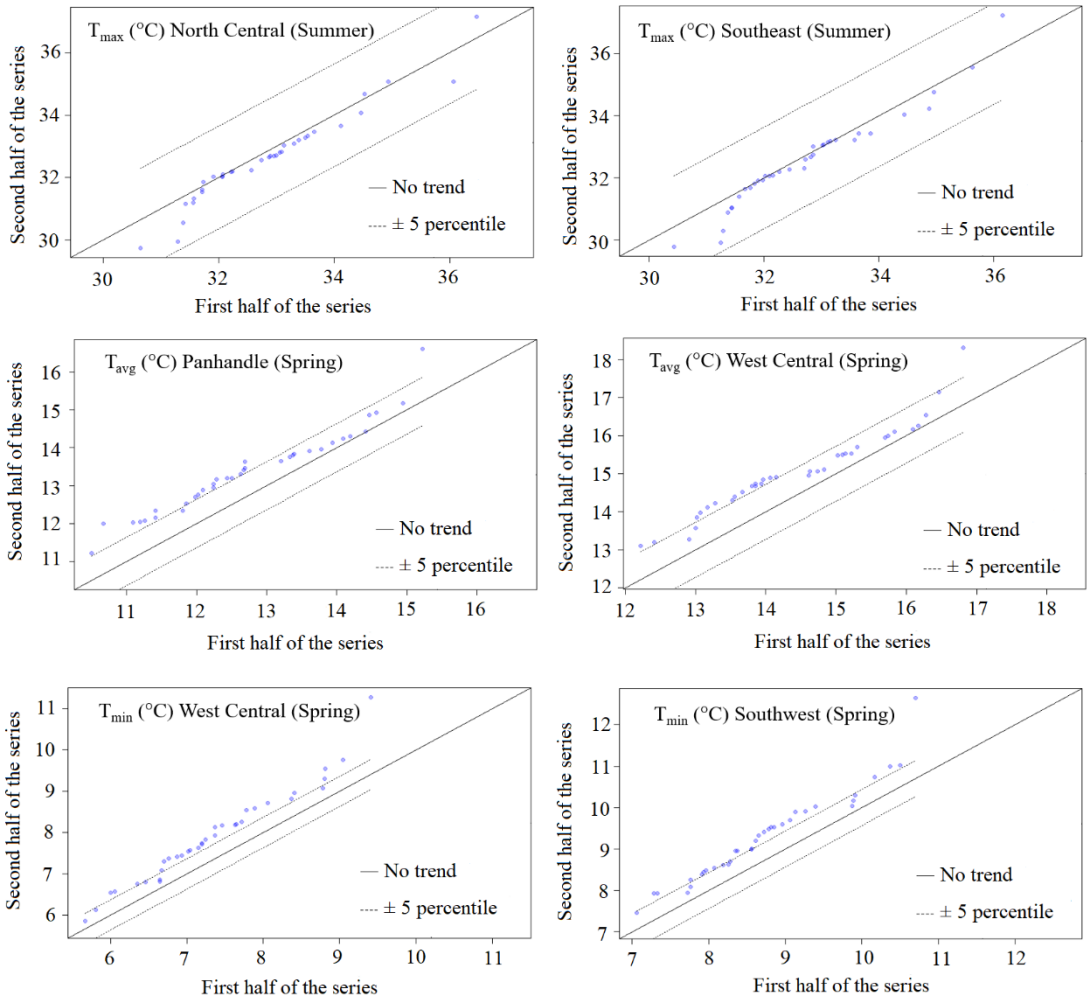

Fig. 2.4. Example ITA tests for temperature trends significant at 95% confidence level.

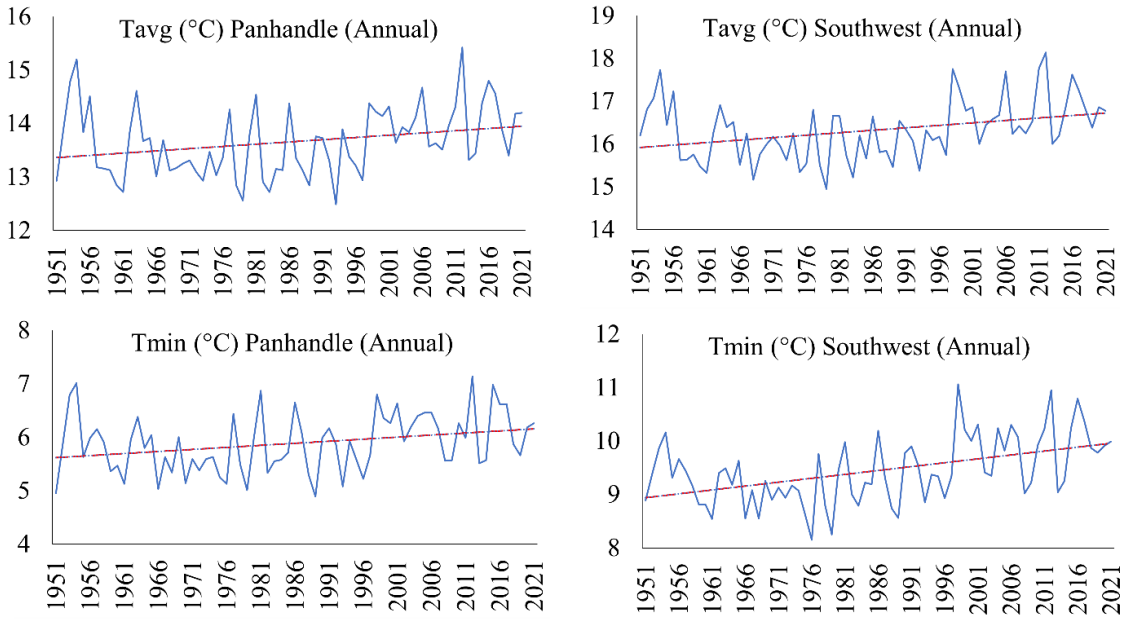

Fig. 2.5. Example significant temporal trends in temperature time series.

2. Precipitation and reference evapotranspiration trends

As shown in Figure 6, P had generally increasing trends annually and seasonally in all the climate divisions, except the Southwest in the fall season, which showed a decreasing trend. The increase in annual P was statistically significant in the North Central, Central, Northeast, and East Central climate divisions. The spring P trend was significant in the Northeast while the winter increasing trends were significant in all the nine climate divisions. Trends in ET_o showed mixed results in both annual and seasonal time scales (Fig 6). Annual ET_o increased non-significantly in the Panhandle, West Central, and Southwest climate divisions ($0.12 \leq p \leq 0.83$), while the rest of the climate divisions experienced a non-significant decline in ET_o ($0.11 \leq p \leq 0.85$) except for South Central climate division where the decline was statistically significant ($p = 0.01$). Most of the climate divisions showed increasing ET_o in spring, fall, and winter, although the increase was statistically non-significant. Statistically significant decreasing summer trends in ET_o were observed in the central and eastern parts of the state.

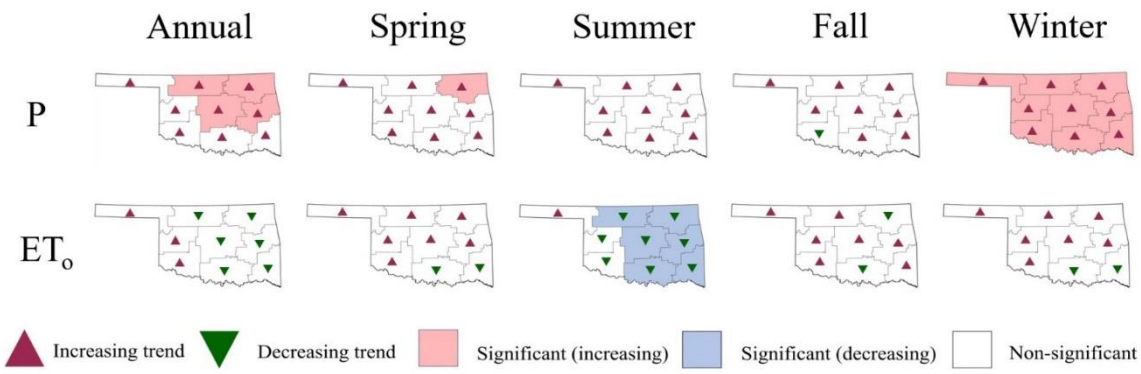

Fig. 2.6. Annual and seasonal trends in P and ETo based on the MMK test. The shaded divisions represent statistical significance at the 95% confidence level ($p < 0.05$).

An east-to-west pattern was observed in the magnitude of increasing average slopes of P both annually and seasonally (Table 3), consistent with the general precipitation gradient (Fig 2). Average Sen's slope of precipitation time series in all time scales increased for eastern, central, and western parts of the state. Annually, eastern Oklahoma had the largest average slopes (2.78 mm/yr), followed by central (2.34 mm/yr) and western (1.06 mm/yr) parts of the state (Table 3). Eastern Oklahoma had the largest average slope for spring (10.73 mm/yr). The average Sen's slopes for precipitation are generally smaller for summer and fall than winter and spring. The average slope for winter season, which had statistically significant increasing precipitation in all the climate divisions, declined from eastern climate divisions (1.01 mm/yr) to central (0.84 mm/yr) and western (0.581 mm/yr) climate divisions, reflecting the westward precipitation gradient.

On average, ET_o increased in the western three climate divisions annually (0.23 mm/yr) and during spring (0.12 mm/yr), fall (0.09 mm/yr), and winter seasons (0.03 mm/yr) (Table 3). Decreasing average ET_o trends were observed in the central and eastern parts of the state for annual and summer season timescales. Panhandle is the only climate division that did not show decreasing ET_o trends. The highest increasing annual ET_o trend was observed in Panhandle (0.42

mm/yr) followed by West Central (0.22 mm/yr), and Southwest (0.05 mm/yr) climate divisions. A similar pattern was observed during the spring season when Panhandle had a positive Sen's slope of 0.19 mm/yr for ET_o followed by West Central (0.14 mm/yr) and Southwest (0.04 mm/yr) climate divisions. Other climate divisions did not show a consistent pattern in either increasing or decreasing trends (Table 3).

The ITA and LSR support the trend results of the MMK and Sen's tests for P and ET_o as well. Most of the points lie above the no trend (1:1) line for statistically significant increasing trends or below the 1:1 line for decreasing trends in seasonal P and ET_o (Fig 7). LSR shows positive slope of annual P in North Central (1.93 mm/yr) and Central (2.76 mm/yr) climate divisions. Likewise, winter P had a positive slope in the Panhandle (0.29 mm/yr) and Southwest (0.43 mm/yr) climate divisions (Fig 8). Similar results were reported by Irmak et al. (2012) in Nebraska, U.S. where they observed statistically significant increasing precipitation and decreasing ET_o trends for a 116-year record on annual scale. Kukal and Irmak (2016) also observed increasing precipitation in counties located in western Oklahoma, which agrees with reports of increasing decadal scale precipitation in the Great Plains region of the U.S. (Garbrecht and Rossel 2002).

Table 2.3. Annual and seasonal Modified Mann-Kendall and Sen's slope tests for precipitation and reference evapotranspiration.

Climate Division	Time Scale	P		ET_o	
		MMK (Z)	SNS (mm/yr)	MMK (Z)	SNS (mm/yr)
Panhandle	Annual	0.558	0.30	1.543	0.42
	Spring	0.019	0.00	1.583	0.17
	Summer	0.744	0.28	0.153	0.02
	Fall	0.645	0.17	0.854	0.08
	Winter	**2.614***	**0.62**	0.000	0.00
North Central	Annual	**2.000**	**2.12**	-0.449	-0.14
	Spring	1.330	0.75	0.511	0.06
	Summer	0.781	0.53	**-2.347**	**-0.29**
	Fall	0.264	0.1	0.561	0.06
	Winter	**3.069**	**0.62**	0.636	0.04
Northeast	Annual	**2.751**	**3.07**	-0.959	-0.29
	Spring	**3.127**	**1.53**	0.129	0.00
	Summer	1.240	0.62	**-2.631**	**-0.42**
	Fall	0.524	0.35	-0.362	-0.04
	Winter	**2.427**	**0.77**	0.715	0.05
West Central	Annual	1.404	1.25	0.783	0.22
	Spring	0.357	0.17	0.993	0.14
	Summer	1.898	0.78	-0.640	-0.08
	Fall	0.114	0.05	0.731	0.11
	Winter	**3.137**	**0.63**	0.596	0.05
Central	Annual	**2.151**	**2.79**	-0.395	-0.08
	Spring	1.363	0.74	0.878	0.11
	Summer	1.697	1.05	**-2.070**	**-0.25**
	Fall	0.421	0.27	0.030	0.04
	Winter	**2.679**	**0.81**	0.650	0.05
East Central	Annual	**2.660**	**3.16**	-0.178	-0.04
	Spring	1.297	0.80	0.859	0.07
	Summer	1.156	0.64	**-2.032**	**-0.22**
	Fall	0.957	0.74	0.347	0.03
	Winter	**2.462**	**1.04**	0.511	0.03
Southwest	Annual	1.529	1.64	0.203	0.05
	Spring	0.989	0.36	0.278	0.04
	Summer	1.778	0.62	-1.030	-0.16
	Fall	-0.226	-0.16	0.430	0.08
	Winter	**2.518**	**0.49**	0.417	0.04
South Central	Annual	1.811	2.26	**-2.417**	**-0.61**
	Spring	1.314	0.69	-1.047	-0.11
	Summer	1.131	0.68	**-4.110**	**-0.44**
	Fall	0.163	0.09	-0.160	-0.01
	Winter	**3.412**	**1.08**	-0.283	-0.02
Southeast	Annual	1.647	2.1	-1.573	-0.44
	Spring	1.280	0.88	-0.471	-0.04
	Summer	0.223	0.17	**-17.061**	**-0.43**
	Fall	0.273	0.22	0.198	0.02
	Winter	**2.852**	**1.21**	-0.079	0.00

* Bold values indicate statistical significance at 95% confidence level for the Mann-Kendall test.

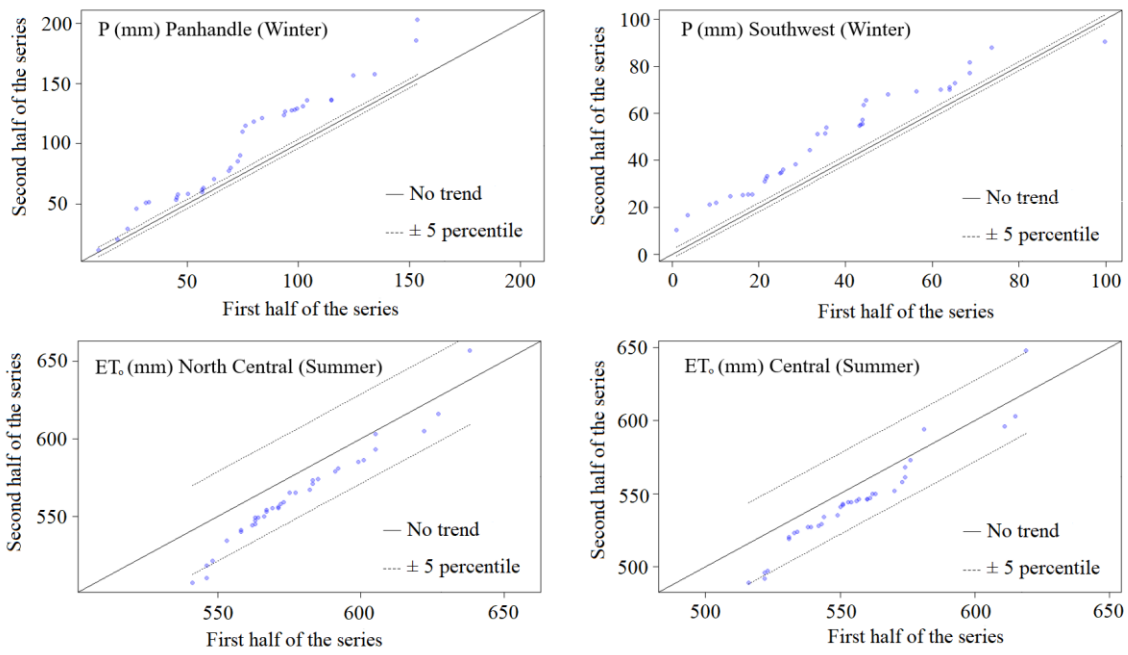

Fig. 2.7. ITA for significant trends in precipitation and reference evapotranspiration at 95% confidence level.

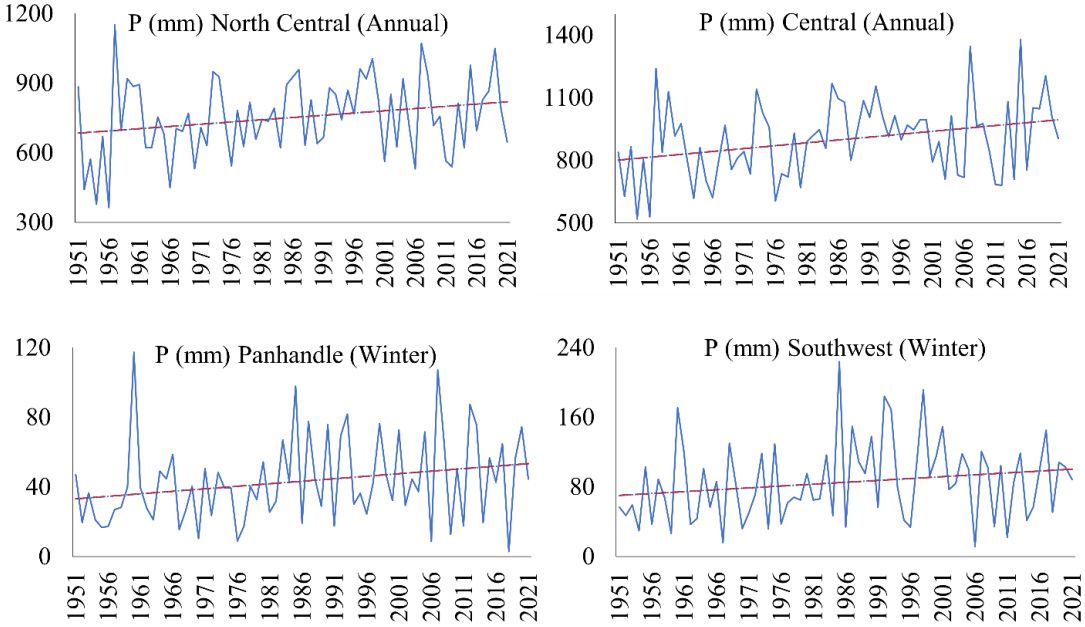

Fig. 2.8. Significant temporal trends in precipitation time series.

2.3.3 Implications of climatic trends

Increasing or decreasing trends in T, P and ET_o have important implications for agricultural production, agricultural water and energy demand, design and operation of water resource systems, and preparedness to manage pests and diseases, among others (Kukal and Irmak 2016 a,b). On one hand, increasing annual and seasonal T_{min} can lengthen the growing season, or they may contribute to favorable conditions for winter crops, especially in the western three climate divisions (the Panhandle, West Central and Southwest). On the other hand, warmer winters may result in survival of pests and growth of invasive and migratory species (Laštuvka 2009; Poland et al. 2021; Skendžić et al. 2021). Increasing trends in T_{max} may lead to excessive heat and deplete soil moisture, which is critical for growing healthy crops (Feng and Liu 2015). Excessive heat can also limit a plant's water uptake by affecting its root development and reducing its ability to transpire (Lipiec et al. 2013). This can impact crop yields, for example in corn and soybeans (Dos Santos et al. 2022), which have been observed in other parts of the world (Lobell et al. 2011; Nicholls 1997; Peng et al. 2004; Tao et al. 2006). Global wheat production is set to decline by 6% per °C of increase in mean temperatures (Asseng et al. 2015; Zhao et al. 2017). For example, at this rate in wheat yields western three climate divisions in Oklahoma can decline by more than 3% (T_{avg} increase of 0.011 °C/yr x 50 yrs = 0.55 °C) in fifty years (i.e., by 2072). Similarly, soybean yield, another major crop in OK, can decline by 1.5% in western OK in the next five decades as it is projected to decline by 3.1% per °C of increase in T (Zhao et al. 2017). Consequently, high temperatures may affect agricultural productivity, farm income, and food security (Battisti and Naylor 2009). According to Zou et al. (2017), surface water areas in Oklahoma are declining at a rate of 0.08 km^2 per year. This has a negative implication for sustainability of practices that depend on surface water, including water supply, hydroelectricity, irrigation, and ranching.

While a generally increasing trend in precipitation may appear to increase renewable water, the ability to store and manage the water for beneficial uses is governed by the intra-annual and intra-seasonal variability of precipitation on short time scales (e.g., daily). Some major issues with increasing precipitation trends across all seasons are the potential disruption in the growing cycles. Extreme precipitation events interspersed with long dry periods in the Southern Great Plains (Kunkel et al. 1999; Mallakpour and Villarini 2017), including western Oklahoma, reduce the ability to capture large runoffs occurring over short time spans (Dawadi and Ahmad 2013; Nepal and Shrestha 2015). Such events can cause flash flooding, which may cause erosion and may result in nutrient and crop loss and damage to property, or even loss of life (Dahl and Xue 2016; Higgins et al. 2011; Teegavarapu 2012).

In Oklahoma, the western climate divisions constitute most of the irrigated agriculture, which depends on limited surface water and groundwater resources. The state's largest share of total irrigated area (42%) is in the Panhandle climate division. The Southwest climate division ranks second with 26% of the state's irrigated area followed by North Central (8%), and the West Central (6%). As illustrated in Fig 8, different climate divisions have witnessed varying severities and durations of drought over the last seven decades. Notably, in the 1950's, extreme to exceptional meteorological droughts frequently occurred in the Panhandle (24% of the time), West Central (27%), and Southwest (18%) climate divisions (Fig 9).

In the last decade, western Oklahoma witnessed droughts that were comparable in severity to the droughts of the 1950's (Fig 9). Record setting temperatures and exceptional drought occurred in the 2011-2012 period (Shafer et al. 2014), causing over $2 billion in agricultural economic losses in Oklahoma (Khand et al. 2017). The drought persisted in the western climate divisions, including the Southwest, halting water delivery to irrigated farms for several years. The drought ended with above-normal precipitation in spring 2015 (Khand et al. 2017). This situation is projected to be exacerbated in western Oklahoma with the reduction of stream flows (OWRB

2012) and increased pressure on fresh groundwater resources in southwestern Oklahoma (Balcombe, 2014). In the Panhandle, where groundwater is the major source of irrigation, the Ogallala aquifer is being depleted to continue supporting irrigated agriculture (Almas et al. 2008). The overdraft during the prolonged drought from 2011 to 2015 resulted in 9 ft of groundwater level decline (Khand et al. 2017). Warmer temperatures and erratic rainfalls compound the challenge of agricultural water availability.

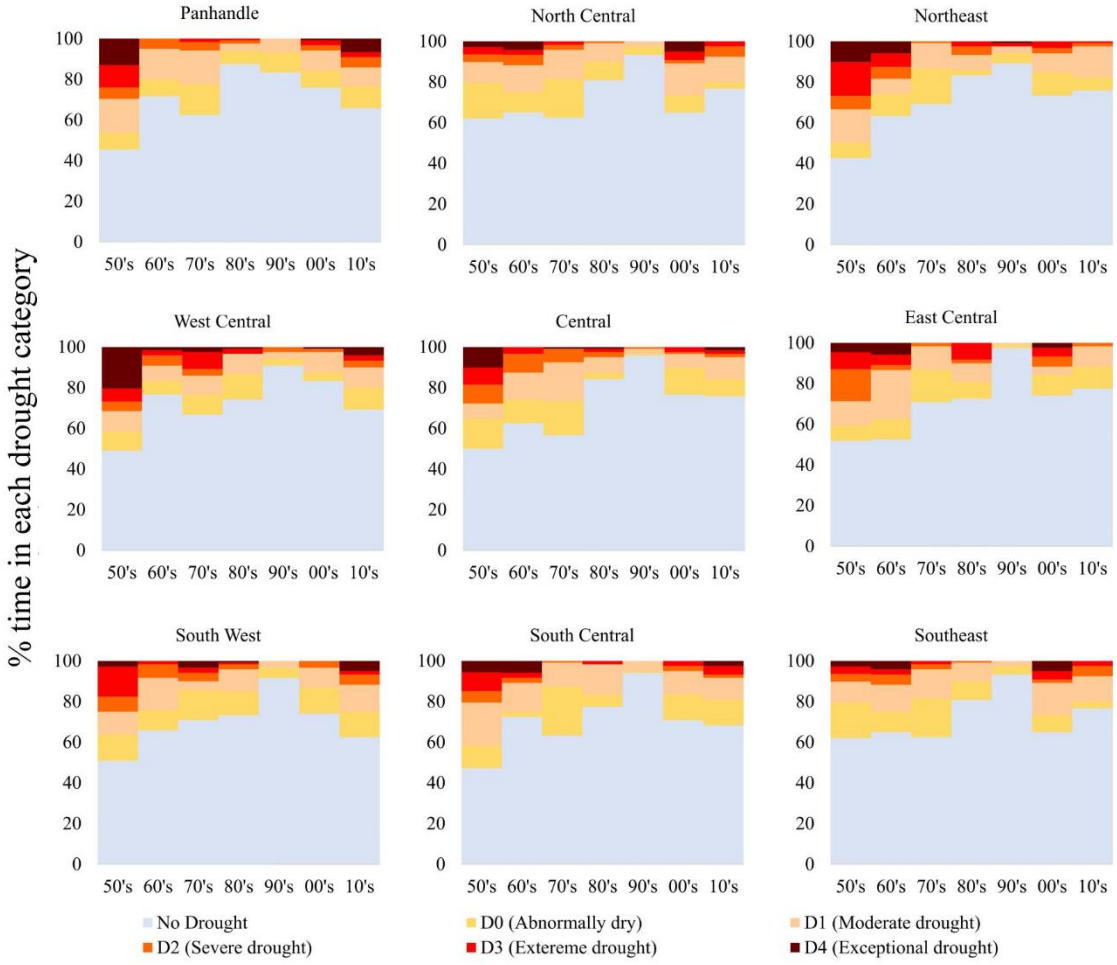

Fig. 2.9. Decadal distribution of droughts in Oklahoma climate divisions

2.4. CONCLUSIONS

This study investigated the annual and seasonal trends of air temperature, precipitation, and reference evapotranspiration in Oklahoma, USA, using 70 years of data and a suite of widely applied tests, including the MMK, SNS, ITA and LSR. The results show increasing temperature gradients from south to north and increasing precipitation gradients from west to east of the state. The spatial gradients for ET_o were not well defined. Temporally, all the climate divisions showed increasing T_{min} trends in both annual and seasonal scales. The largest slopes of these increases were in the spring, fall, and summer seasons. All the climate divisions showed increasing T_{max} and T_{avg} trends except for summer seasons. Statistically significant trends were observed mainly in T_{min}, and T_{avg}, on annual and seasonal basis. Predominantly western climate divisions had the most increasing temperatures both annually and seasonally. Precipitation showed increasing trends in all climate divisions for most of the timescales. Statistically significant trends were observed in P in all the climate divisions during winter season. ET_o showed mixed trends spatially and temporally while statistically significant decreasing ET_o trends were observed in the central and eastern parts of the state during the summer season. It is important to observe the magnitudes of trends and incorporate these into planning and management of water resources and agricultural infrastructure in the face of recurring severe to exceptional droughts.

CHAPTER III

STATION ARIDITY IN THE WEATHER MONITORING NETWORKS: EVIDENCE FROM THE OKLAHOMA MESONET

3.1. INTRODUCTION

Accurate estimation of water required for irrigation is critical for efficient agricultural water resources planning, management, and decision-making. A common approach to quantify crop water requirement is to estimate crop evapotranspiration (ET) using the reference evapotranspiration (ET_{ref}) concept. ET_{ref} is calculated by estimating the ET of a reference surface defined as "a uniform surface of dense, actively growing vegetation having specified height and surface resistance, not short of soil water, and representing an expanse of at least 100 m of the same or similar vegetation" (ASCE, 2005). For accurate estimation of ET_{ref} at a given location, it is recommended that the site be surrounded by well-watered vegetation, preferably clipped grass, or alfalfa or grass-legume maintained at less than 0.5 m height to represent reference surface condition (ASCE, 2005).

The standardized Penman-Monteith (PM) method (Allen et al., 1998; ASCE, 2005, 2016) is widely applied by weather monitoring networks to estimate ET_{ref}, using a number of weather parameters including T, wind speed (W), R_n, and vapor pressure (e). To estimate ET_{ref} a fetch ratio of 100 times the height of T, W, and RH sensor is recommended (Allen, 1996; ASAE, 2004) so that the incoming flux represents irrigated setting. For agricultural purposes T and RH sensors

are usually mounted at 1.5 m and W sensors at 2 m height above the ground surface. Therefore, a well-watered fetch of 150-200 m is needed for ET_{ref} estimation. However, such an expanse of vegetation is oftentimes not available at mesoscale weather monitoring stations, which are sited according to different requirements depending on the primary functions of the monitoring network. For example, a station with the intended use of integrated pest management should be located between crops which may not necessarily be of specified height or irrigated, e.g., orchards and groves (ASAE, 2004). Another example is an aviation meteorological station, which should record observations at individual local aerodrome site (WMO, 2018).

Oklahoma Mesonet (hereafter Mesonet) stations are sited on a variety of lands in terms of ownership and maintenance, including academic institutions, agricultural research stations, private land, federal/city/state land, and airports. An "ideal" site is not always available because many stations are sited after making arrangements with cooperative private landowners or because of different uses of data, which may need variable and sometimes contrasting siting requirements. Shafer et al. (1993) presented guidelines to select sites for Mesonet stations, including accessibility by vehicle and representativeness of as large an area as possible. Therefore, stations are generally sited away from water bodies, dams, irrigated areas, and forests so that their influence on the observations is minimized (Fiebrich et al., 2010; McPherson et al., 2007). Most Mesonet stations are installed on native vegetation where rainfall is the only water source for ET. Therefore, rainfall amount, frequency, and distribution are key in determining if the surface condition is approaching reference or not (Itenfisu et al., 2002). Previous research has documented the impact of surface conditions on observed T, RH, and W. De Vries et al. (1961) compared meteorological measurements including T and RH using three stations in an irrigated area (6 to 7 km2) and one station in an adjacent dryland area in Australia. The reported average differences were 1-2 °C for T and 5-10 % for RH during the summer for a period of four weeks. Davenport et al. (1967) conducted experiments in Sudan to observe T, W, and vapor pressure

deficits (VPD) on a 17 km transect of a 300 m wide cotton field and found lower T, W, and VPD on the leeward edge than windward edges. At a desert site in Idaho, USA, T_{avg} was 3 °C greater and ET was 20% larger than at the center of an irrigated field within a 50 km transect (Burman et al., 1975). Likewise, Allen et al. (1983) reported greater T and lower RH at two arid sites compared to three irrigated stations in Idaho. The ET_{ref} at the arid sites was 17% greater for the season and 21% for the month of July. Using data from eight weather stations, Ley et al. (1994) reported that, on average, maximum and minimum air temperatures (T_{max} and T_{max}) were 1.8 °C and 1.1 °C greater in arid sites during July and 0.9 °C and 0.7 °C greater during the growing season. Vapor pressures were 6% smaller in July and 7% smaller in the growing season. ET was 20% and 19% greater in July and over the growing season, respectively. W was also found to be greater in the dry locations than over irrigated surface.

Station aridity effects caused by non-reference surface conditions have important implications for weather-based agricultural water management. Herein, we characterize station aridity across the Oklahoma Mesonet, which provides estimates of ET_{ref}, among other weather parameters, to facilitate weather-informed irrigation decisions in the state of Oklahoma, USA. Using a 20-year record of daily weather data, we calculate mean dew point deviation ($MDD = T_{min} - T_{dew}$), maximum relative humidity (RH_{max}), and NDVI to characterize station aridity. The paper contributes to a better understanding of the prevalence and spatiotemporal characteristics of weather station aridity across the Mesonet with implications for similar multi-purpose weather monitoring networks in the USA and around the world.

3.2. MATERIALS AND METHODS

3.2.1. THE OKLAHOMA MESONET

The Oklahoma Mesonet (hereafter Mesonet) is a network of 120 active environmental monitoring stations spread across the state of Oklahoma. These automated stations are designed to report

various weather parameter data in near real time, providing an invaluable infrastructure to capture mesoscale climate features. The Mesonet serves multiple purposes, including weather forecasting, emergency management, wildfire management, environmental research, transportation, and agriculture, among others (McPherson et al., 2007). Since starting operation in 1994, the network has recorded most weather parameters such as T, precipitation (P), RH, W, and air pressure, among others, at 5-minute intervals while also providing average soil temperature and soil moisture data at 15-minute and 30-minute intervals, respectively (Brock et al., 1995; McPherson et al., 2007). The Mesonet estimates ETref based on the ASCE standardized reference evapotranspiration approach (ASCE, 2005), which requires the weather parameters to be measured over reference surfaces.

3.2.2. DATA AND QUALITY ASSURANCE

We used archived daily data from a select number of Mesonet stations (Fig. 3.1) for the period of 1 January 2000 to 31 December 2019 (20 years). The number (initially 142) and location of some Mesonet stations have changed over time since 1994 because of retiring stations and/or moving them to a new location for various reasons. For stations that were moved to a new location, Mesonet merges the data obtained from the old site with data from the new location. We excluded these stations because the microclimate of an area impacts the ET process and therefore data collected from such shifted stations would not be reflective of a single station ET. Moreover, 28 stations launched after 2000 were not included in our analysis due to their relatively short length of data. Baddour et al. (2007) recommended a 10% threshold to fill the gaps of missing values in weather datasets. Thus, stations with more than 10% missing data were also removed, except for two stations of Tipton and Altus in southwestern OK, which had 10.4% and 10.2% missing data, respectively. This process resulted in selection of 83 Mesonet stations for further analysis.

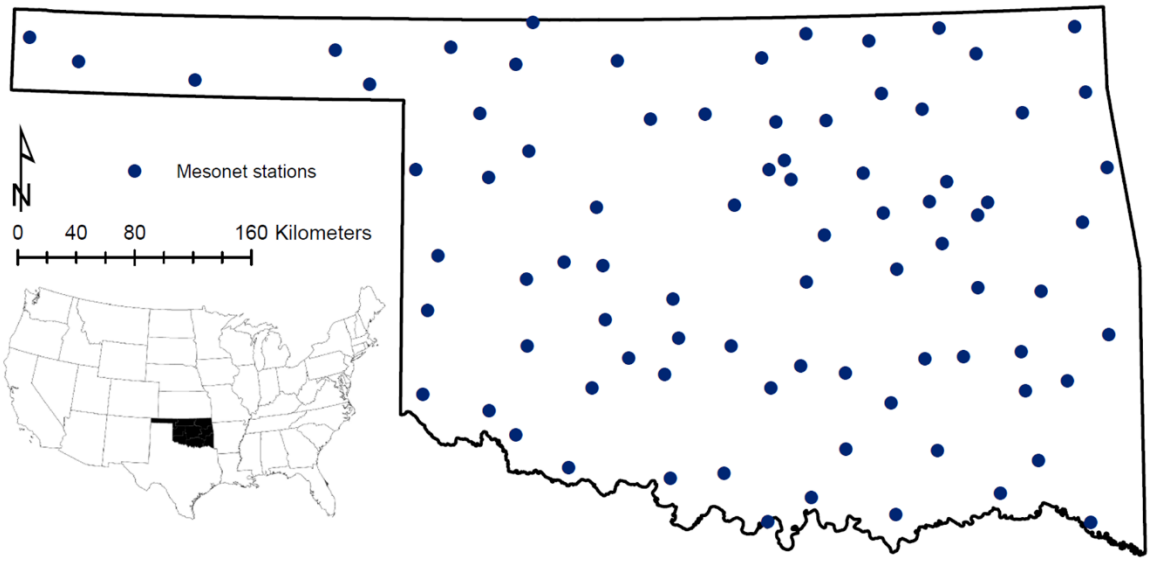

Fig. 3.1. Location of the 83 selected Mesonet stations in Oklahoma, US.

Mesonet employs both automated and manual quality assurance (QA) checks to ensure collection of research quality data. An automated QA software performs a variety of tests on the observed weather parameters to identify erroneous data. These tests include range tests, temporal checks, spatial checks, like instrument checks, and adjustment tests. If the QA software identifies a problem, it flags the observation(s) in a daily QA report which lists the output from the automated QA tests (McPherson et al., 2007). The manual QA process includes inspection of the auto-generated report by a meteorologist who determines whether or not the recorded data represent a real meteorological phenomenon (Fiebrich et al., 2001). Although the combination of automated and manual checks results in high data quality, we performed a number of additional checks to ensure that there is no error in the reported daily values of T_{min}, T_{min}, P, and RH_{max}. We searched for days with $T_{min} > T_{max}$, $P < 0$, and where $RH_{max} < 0$ or >100. Mesonet calculates dew point temperature (T_{dew}) from T and RH. Therefore, resolving errors in T and RH data eliminates false T_{dew} values. Allen et al. (2011) recommended a careful examination of the data collected from non-reference weather stations before estimating ET_{ref}. Therefore, we also applied QA procedures recommended by the ASCE (2005) and Allen et al. (1998). We followed their guidelines to

calculate the extreme ranges of daily solar radiation (R_S), RH_{max} and average W and to assess the integrity of the data falling between the extremes. For each Mesonet station, we plotted measured R_S against the theoretical clear sky solar radiation (R_{SO}) calculated using the equations that account for the influence of sun angle, turbidity, atmospheric thickness, and precipitable water (see an example in Figure S1 in Supplementary Material (SM)). We checked if the measured R_S was consistently above or below the R_{SO} curve by more than 3 to 5%. Such an observation could indicate a problem with the sensor calibration. This approach was also used by Itenfisu and Elliott (2002) in a study in which they adjusted the Mesonet's measured R_S values using the procedures mentioned in (Allen, 1996). We adjusted the daily R_S values of all stations (i.e., $R_{S(adj)}$) using the University of Idaho's REF-ET software version 4.1 which adjusts R_S values by using unique multipliers determined for each 60-day period (Richard G. Allen, 2016).

We examined wind and humidity data by first checking for consistently low W values (< 0.5 m/s), which indicates failed bearings of anemometers. There were some days in all the stations when W at 2 m recordings were less than 0.5 m/s but they were not consistent and therefore, W dataset was not altered in any way. We also plotted daily RH_{max} values from all stations to detect potential sensor calibration errors (an example is shown in Fig. S2 in SM). These checks did not result in exclusion of any data. Fig. S3 in SM illustrates the QA steps implemented in addition to the QA conducted by the Mesonet. Upon completion of the QA procedure, we selected 83 Mesonet stations for this study as shown in Figure 1.

3.2.3. STATION ARIDITY

We used mean dew point deviation (MDD), maximum relative humidity (RH_{max}), and NDVI across the state over the 20-year period to distinguish between reference and non-reference conditions. MDD refers to the difference between T_{min} and T_{dew}. We used MDD as an indicator of station aridity following (Temesgen et al., 1999). In arid regions and under non-reference

conditions where sufficient water is not available to meet the evaporative demand of the atmosphere, T_{min} does not approach T_{dew} even in the early morning hours, resulting in a positive MDD value. It has been observed that there is a difference of 2 to 5°C between T_{min} and T_{dew} even if reference conditions are present (ASCE, 2016). This is attributed to continuous mixing of warm and dry air from the surrounding (Temesgen et al., 1999). Therefore, we used the percent days in which MDD > 2°C (IMDD) as an indicator of station aridity.

RH_{max} will often approach 100% in humid regions or at sites where reference conditions prevail. In the absence of problems like sensor malfunction or calibration issues, site aridity can result in RH_{max} consistently falling below 100%. In this study, we adopted 80% as the threshold to designate arid condition at Mesonet stations. Since the QA of the data did not indicate sensor problems, percent days with RH_{max} < 80% (i.e., IRH) was used as our second indicator to characterize station aridity.

Reference conditions can also be assessed by calculating NDVI values around a station. Various factors including the plant growth stage and availability of water can affect reflectance characteristics of surfaces. A low NDVI indicates lack of actively transpiring vegetation i.e., non-reference conditions. For example, barren lands and sparsely vegetated surfaces typically have NDVI values less than 0.4. An actively growing plant with sufficient water supply from the soil has a high NDVI. In sub-humid and humid regions natural vegetation is greener because the water requirement is usually met, resulting in NDVI values approaching 1.0.

In this study, percent days with NDVI < 0.4 (INDVI) is used as our third indicator of station aridity. Such an approach was used by Blankenau et al. (2020) to filter stations that were not in reference condition during the growing season. We used MODIS (Moderate Resolution Imaging Spectroradiometer) 500 m resolution 16-day imagery from 2000 to 2019 to calculate NDVI around each station. Following Blankenau et al. (2020), average NDVI for a station was

computed as the average NDVI over areas within 500 m and 2 km radii of each station to account for the influence of local and regional scale aridity on the fluxes received by the sensor. Thus, NDVI denotes average NDVI throughout this paper.

3.2.4. SPATIAL AND TEMPORAL ANALYSIS

We analyzed the spatiotemporal variation of Mesonet station aridity based on MDD, RH_{max}, and NDVI to characterize the pattern, extent, and timing of station aridity. For the spatial analysis, we divided the state into western and eastern zones. The western zone consists of the 30 western counties and accounts for 88% of the state's irrigated area. The temporal analysis was conducted on annual and seasonal scales. We chose winter (WI), spring (SP), summer (SU), and fall (FA) as the four meteorological seasons in a year based on the annual temperature cycle. Spearman's correlation coefficient was used to measure the strength of association between the indicators and precipitation. The strength of correlation is given as: very weak (0.00 - 0.19), weak (0.20 - 0.39), moderate (0.40 - 0.59), strong (0.60 - 0.79), and very strong (0.80 - 1.00) (Myers et al., 2010; Spearman, 1961). The station aridity indicators were also evaluated with respect to different drought categories (D0: abnormally dry, D1: moderate drought, D2: severe drought, D3: extreme drought and, D4: exceptional drought) of the US Drought Monitor (Svoboda et al., 2002).

3.3 RESULTS AND DISCUSSION

The spatial variation of the average (2000-2019) magnitude of MDD, RH_{max}, and NDVI from southeast to the OK Panhandle generally follows the precipitation gradient (Fig. 3.2). Larger magnitudes of MDD are observed for Mesonet stations in western Oklahoma, which is drier (annual average rainfall: 675 mm), as compared to the corresponding values in the wetter eastern part of the state. The maximum and minimum values of average MDD across all stations are 3.3 °C for Kenton station located in the OK Panhandle and -1.6 °C for Wister station in the southeast. In total, 17 stations had average MDD < 0 all of which are in eastern OK. As expected, larger

values of RH_{max} and NDVI are observed in eastern OK. Southeastern OK receives up to 1815 mm of rainfall annually and therefore the stations are expected to have larger magnitudes of average RH_{max} and NDVI as sufficient water is available for transpiring green vegetation. The maximum 20-year average RH_{max} of 96% was found at Wister station in the southeast and the minimum of 83% in Medicine Park and Cheyenne stations in western OK. Similarly, the maximum average NDVI of 0.64 was found at Cookson station in eastern OK and the minimum of 0.25 at Kenton station in the Panhandle. Overall, the three variables show strong (RH_{max} ~ NDVI: 0.76 and MDD ~ NDVI: -0.76) to very strong correlation (RH_{max} ~ MDD: -0.98) with each other across all the stations.

It is worth noting that some Mesonet stations behave anomalously in terms of the magnitudes of MDD and RH_{max} compared with neighboring stations. For example, Chickasha station located in western OK had a smaller average MDD (0.1 °C) and a larger RH_{max} (91%) compared with the neighboring Washington station's average MDD (0.8 °C) and RH_{max} (90%) despite receiving lesser rainfall (827 mm vs 910 mm). Similarly, moving further southeast from Washington station, average MDD and average RH_{max} for Byars station increased to 1.6 °C and decreased to 87%, respectively, contrary to the general pattern of declining average MDD and increasing average RH_{max} in eastern Oklahoma. Such anomalous behaviors are mostly observed at stations located between the 97th and 99th meridians, which is a transition zone between the humid eastern US and the arid western regions (Seager et al., 2018; Webb, 1931). Further, land management around a station can play an important part in a station's aridity as compared with its surroundings because of the influences of the fluxes received by the sensor.

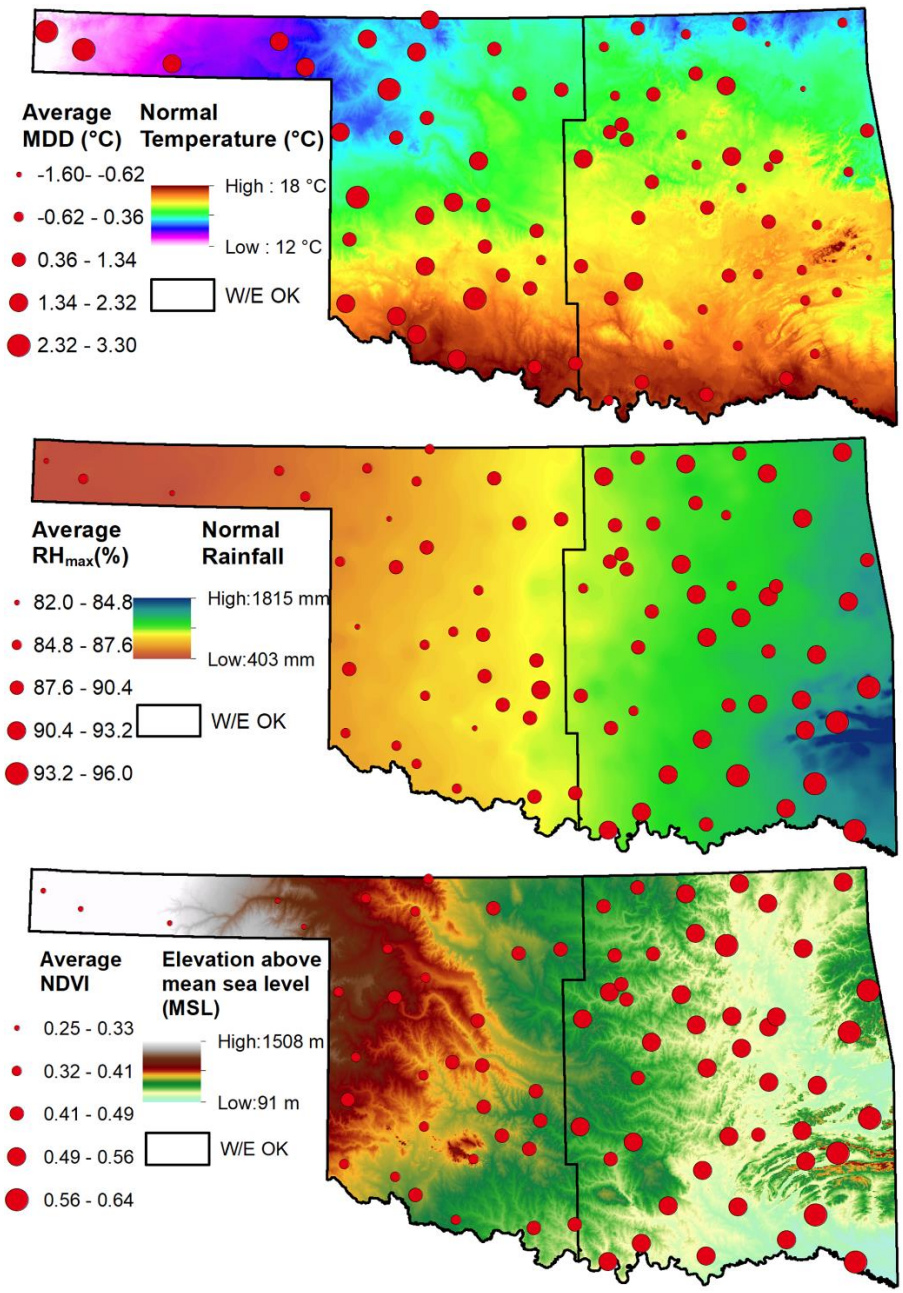

Fig. 3.2. Spatial variability of average MDD, RH_{max} , and NDVI across OK. Base maps represent normal (1990-2020) Temperature and Precipitation and elevation from PRISM (Daly et al., 1994).

Spatiotemporal characteristics of station aridity in the 34 Mesonet stations located in western OK underscore the prevalence of this phenomenon in this region, where accurate ET_{ref} data are

critically needed to guide water conservation through weather-informed irrigation decisions. MDD, RH_{max}, and NDVI vary considerably from season to season across the western stations (Fig. 3.3). Seasonal averages of MDD for the 34 western stations illustrate that summer seasons usually have the highest average MDD (2.97 °C) followed by fall (1.37 °C), spring (1.35 °C), and winter (0.57 °C). Also, summer seasons have the least average RH_{max} (85.74%) followed by winter (86.57%), fall (87.18%), and spring (87.49%). It is during spring and summer that the natural vegetation becomes greener with average NDVI being 0.52 and 0.56, respectively. As leaves begin to senesce in fall, we observe a decline in average NDVI to 0.48. A consistently low average NDVI of 0.34 is observed during winter seasons because natural vegetation becomes dormant.

Droughts compound the station aridity effect by increasing MDD and reducing RH_{max} with visible impacts on the vegetation as indicated by low NDVI values for areas surrounding the stations. The maximum seasonal MDD of 11.92 °C (i.e., 8.95 °C greater than the summer average) occurred in summer 2011, which was the driest season in the 20-year study period with only 85 mm of rainfall. In this year, the majority of western OK experienced extreme (D3) to exceptional (D4) drought. The minimum MDD for summer 2011 was 5.82 °C, which is 2.85 °C greater than the 20-year summer average MDD for western OK. In the same season, maximum RH_{max} was 77% and minimum was 57%, both of which are far less than the 20-year average RH_{max} for the summer season. These values indicate elevated levels of station aridity, which is also reflected in low NDVI values with maximum NDVI being 0.46 and a minimum of 0.22 in summer of 2011. A gradual decline of MDD in summer seasons is observed after 2011 as the prolonged drought weakened. Expectedly, an opposite pattern is seen for RH_{max} and NDVI both of which increased after summer 2011. Conversely, summer 2017 was a relatively wet season for western OK with 272 mm of rainfall. We observe maximum MDD of 2.31 °C and a minimum of -0.58 °C. Most of the stations (29 out of 34) had MDD < 2 °C. In the same season, we observe

maximum RH_{max} of 96% and a minimum of 82%. Similarly, the maximum NDVI was 0.63 and minimum was 0.30. It is noteworthy that relatively large rainfall (276 mm) in spring 2017 helped increase soil moisture for later use in the summer season, contributing to lower MDD and larger RH_{max} and NDVI.

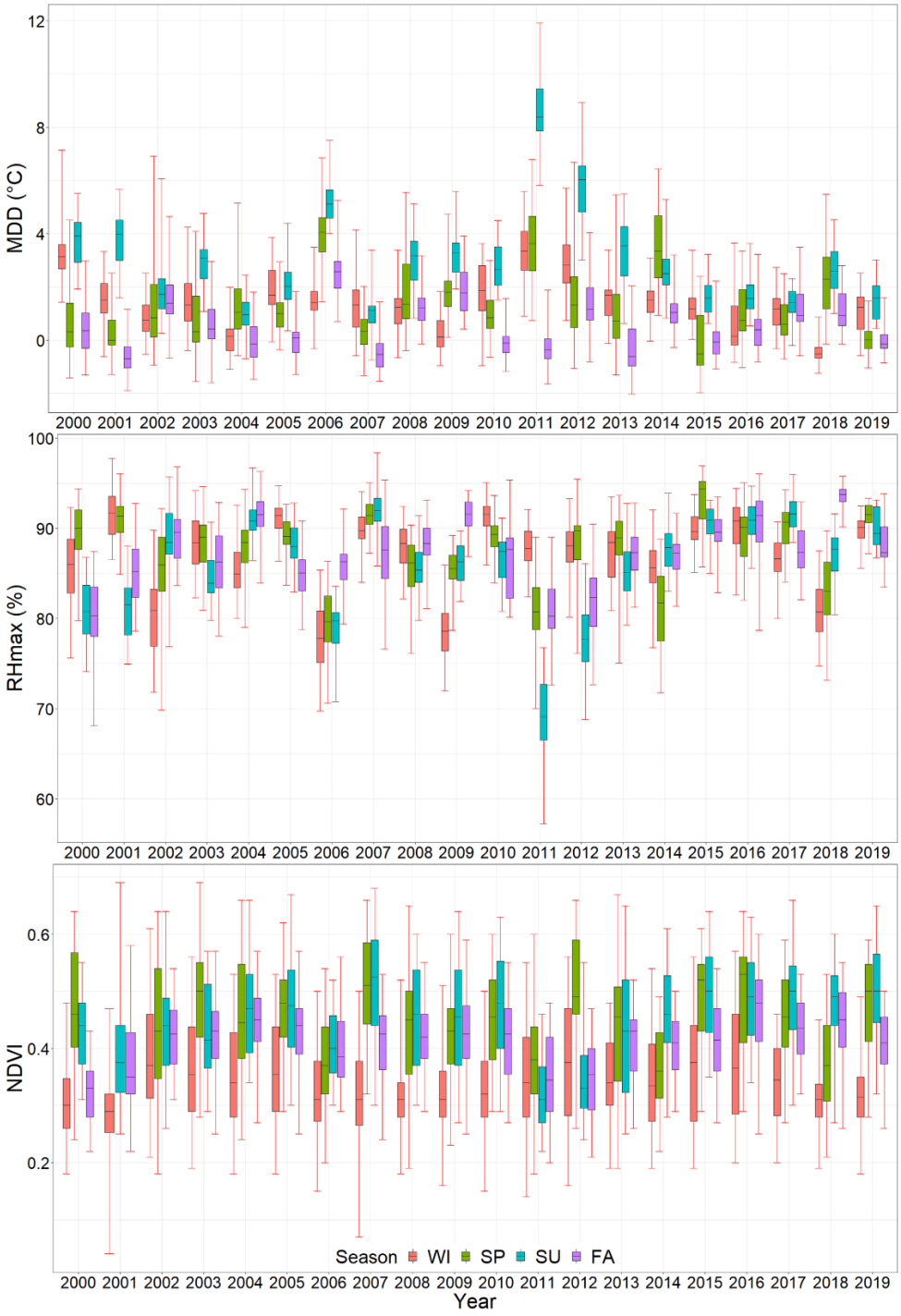

Fig. 3.3. Seasonal variation of MDD, RH_{max}, and NDVI in 34 stations located in western OK.

Visual representation of MDD from 2000 to 2019 across the Mesonet at the spatial scale of individual stations (Fig. 3.4) illustrates a relatively darker shade for the western stations,

indicating a larger MDD, and generally lighter shade for the eastern stations. The gradient of darker and lighter shades is consistent with the variation of the amount of rainfall recorded at the stations. The effect of droughts on MDD is clearly visible in darker vertical shades in the summer of 2006, 2011, and 2012. Therefore, arid sites such as in western OK require correction of station aridity before estimating ET_{ref} because T_{min} cannot be assumed to reach T_{dew} (Cai et al., 2007). Combined effects of rainfall, occurrence of droughts, land surface conditions, and wind characteristics contribute to the emergence of horizontal patterns of dark or light shade based on the differences of MDD between stations that receive similar amounts of rainfall. The differences between MDD for the western and eastern regions increase during summer and fall seasons. Comparable patterns of spatiotemporal variability are observed for RH_{max} and NDVI (Fig. S4 and S5 in SM).

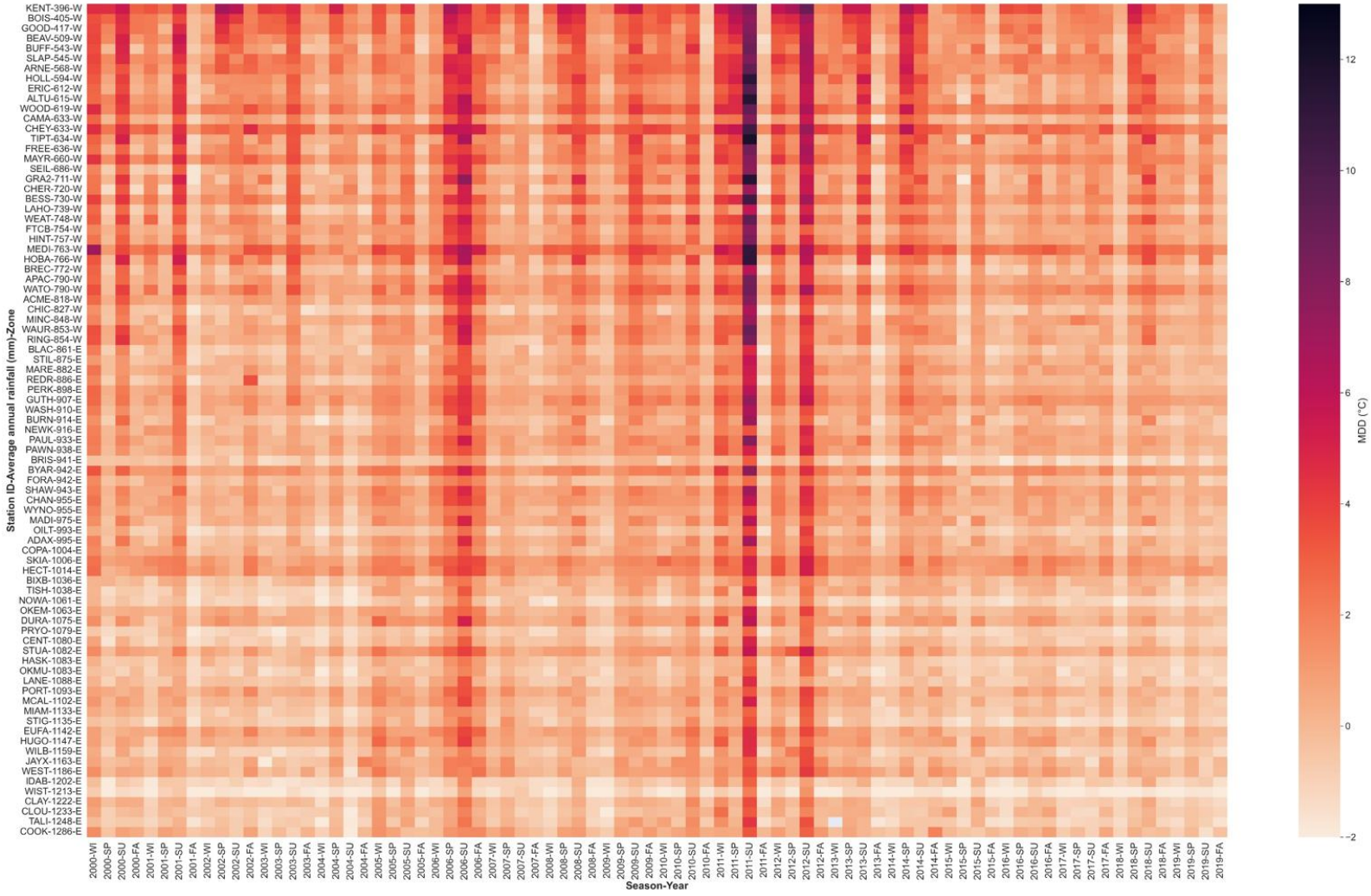

Fig. 3.4. Spatiotemporal variation of seasonal MDD in western (W) and eastern (E) stations sorted ascendingly based on rainfall.

We evaluated relative dryness of Mesonet stations in western OK based on the relationship between mean monthly MDD and P/ET_{ref} (Fig. 3.5). P/ET_{ref} values closer to and greater than unity indicate that the rainfall is equal to the ET demand of the atmosphere and a reference condition can be assumed to exist. By contrast, values closer to zero indicate that the rainfall is much less than the ET demand, meaning reference does not exist. Negative MDD values were excluded because either they represent reference surface condition or cold air temperatures. In western OK, P/ET_{ref} exceeded 1 in 13% of the months during the 2000-2019 period, of which 96% had MDD < 2 °C. Thus, the threshold of MDD = 2 °C for the occurrence of reference condition is justified. Monthly MDD can reach 13 °C when $P/ET_{ref} = 0$. It decreases as P/ET_{ref} approaches 1 and for values of $P/ET_{ref} > 1$. Fig. 5 displays a large scatter of points for P/ET_{ref} close to 0, indicating greater variability in monthly MDD at stations that receive a small amount of rainfall in western OK. This relationship is similar to observations from 26 stations across the US (Allen, 1996) and from the CLIMWAT dataset from eight different countries whose climate conditions ranged from arid to humid (Temesgen et al., 1999). The results indicate that MDD decreases with increasing relative wetness (P/ET_{ref}) and this phenomenon can be observed in different climates globally (Allen, 1996; Temesgen et al., 1999).

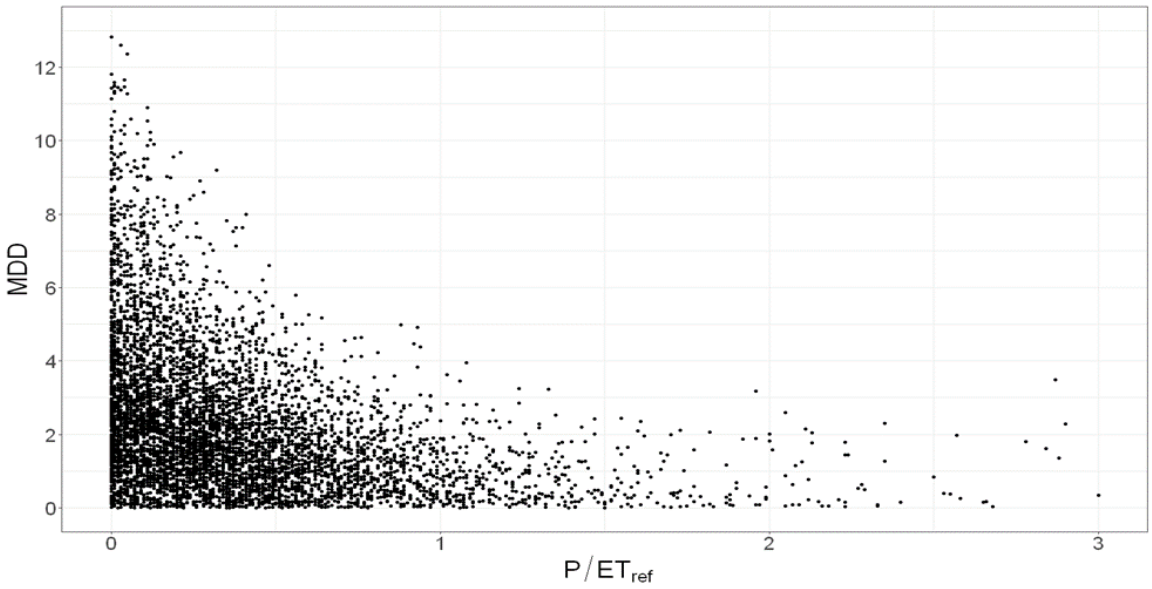

Fig. 3.5. The variation of mean monthly MDD with P/ET_{ref} plot for Mesonet stations located in western OK.

3.3.1. SPATIAL VARIABILITY OF ARIDITY INDICATORS

The average I_{MDD} (i.e., percent days with MDD > 2°C), I_{RH} (i.e., RHmax < 80%), and I_{NDVI} (i.e., % time NDVI < 0.4) for all 83 Mesonet stations during the 20-year study period are 30%, 17%, and 35%, respectively. This corroborates the general prevalence of station aridity across the Mesonet. However, the spatial distribution of aridity indicators is uneven between eastern and western zones. Most stations (31 out of 36) that had above average station aridity based on the I_{RH} were in the western zone (Fig. 3.6). Similarly, 32 out of 37 stations that had above average aridity based on the I_{MDD} were in western OK. The minimum and maximum percentages of the study period under aridity effect, respectively, were 8% and 54% for I_{MDD}, 3% and 36% for I_{RH}, and 0% and 92% for I_{NDVI}. The minimum I_{RH} value (3%) was found at Idabel and Wister stations (3%) in far southeastern OK. The maximum values are for Medicine Park (36%), Cheyenne (36%), and Kenton (35%) in the southwest and the OK Panhandle. Medicine Park did not have a single day in summer 2011 when MDD was below 2 °C. These results are similar to the observations in

Central Arizona where MDD was reported to exceed a threshold of 3 °C more than half (54%) of the time during the 1999-2001 period (Jia et al., 2004).

I_{NDVI} shows a similar pattern as the other two indicators. The maximum I_{NDVI} is 92% and 90% for Kenton and Boise City stations, respectively, both of which are located in the far west OK panhandle. The minimum I_{NDVI} was 0.22% at Broken Bow and the second smallest I_{NDVI} value was 0.68% at Cloudy station, both of which are in southeastern OK. The wide ranges of percent days with aridity effect (46%, 33% and, 90% for I_{MDD}, I_{RH} and I_{NDVI}, respectively) imply that large spatial variations exist among Mesonet stations and that the effects of aridity are highly dynamic across the state.

All three indicators show a strong to very strong monotonic correlation with average annual P represented by the Spearman correlation coefficients of -0.80, -0.79, and -0.76 for I_{MDD}, I_{RH}, and I_{NDVI}, respectively. Very strong correlations of 0.83, 0.85, and 0.82 were also observed with station elevation. I_{MDD} had a very weak correlation (-0.11) with T_{avg}. I_{RH} and I_{NDVI} had weak correlations of -0.21 and -0.20, respectively, with T_{avg}. Weaker correlations imply that variation in average temperature has little effect on station aridity in Oklahoma compared with P and elevation. This is most likely due to the small range of 20-year T_{avg} (12.78 °C – 17.22 °C) in the state. Strong correlations with P were expected as it provides water to the natural vegetation to actively transpire and has a steep gradient from southeast OK to Panhandle, thereby increasing the RH_{max} and NDVI and decreasing MDD.

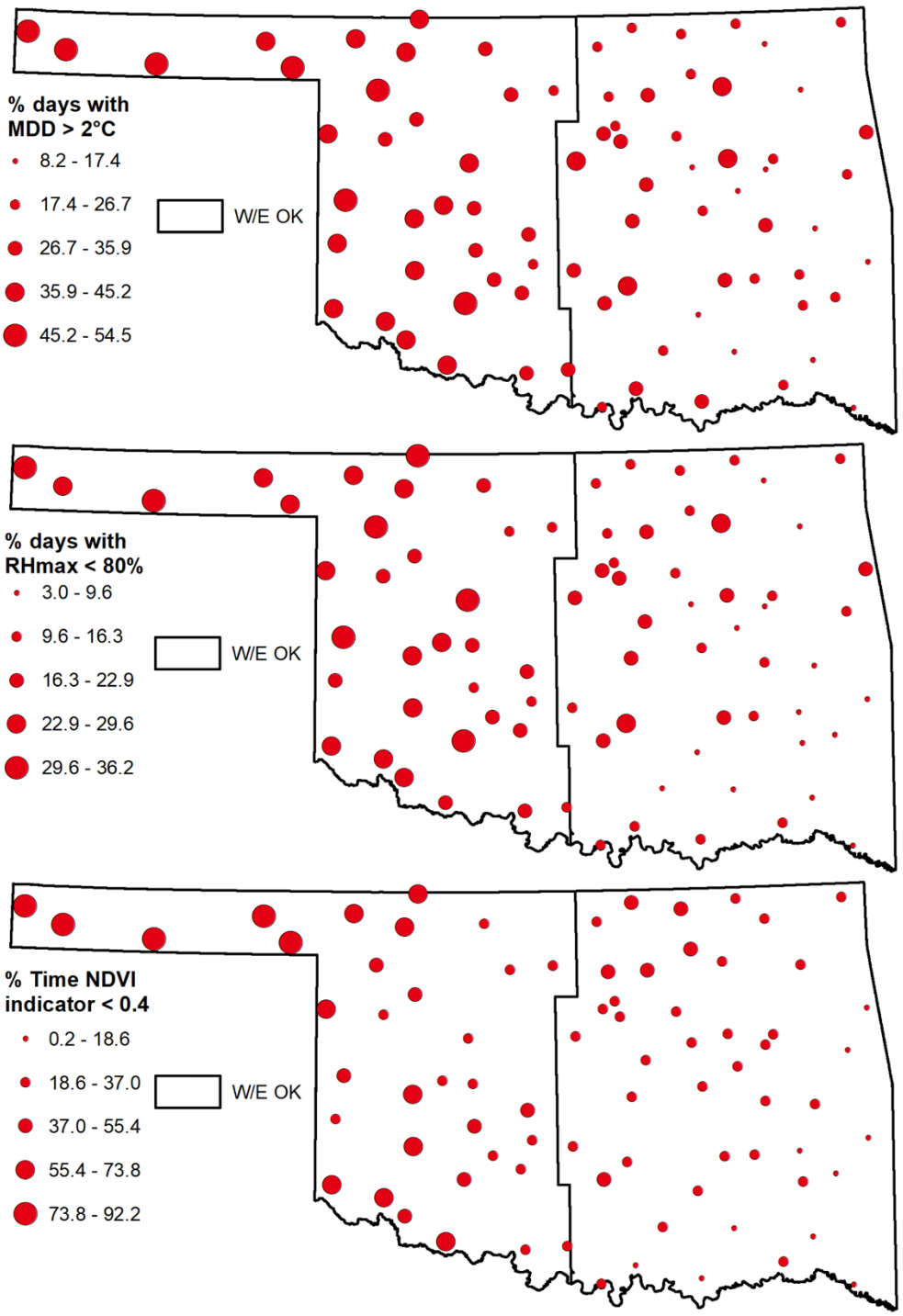

Fig. 3.6. Spatial variation of I_{MDD}, $I_{RH,}$ and I_{NDVI} at Oklahoma Mesonet stations.

The thresholds of < 80% for the RH_{max} indicator, > 2 °C for the MDD, and < 0.4 for the NDVI were adopted from previous studies (Allen, 1996; Blankenau et al., 2020), which ascertain that

these thresholds will generally be exceeded on dry days but not always. For example, Jia et al. (2004) frequently observed MDD > 3 °C in summers in a well-irrigated Alfalfa field in reference condition. Also, it is possible that one indicator exceeds the threshold while the others do not. There are several instances in our dataset where RH_{max} > 80% and MDD > 2 °C. Therefore, these indicators should be used to gather a general sense of station aridity and not as the absolute thresholds. Despite these caveats, the results bear important implications for agricultural water management by illustrating the conditions that lead to overestimation of ET_{ref} in arid/semi-arid agricultural areas which can also affect the reliability of ET_{ref} forecasts (Vanella et al., 2020).

The economic benefit of the information provided by the Oklahoma Mesonet from 2006 – 2014 was estimated to be $183.4 million (Ziolkowska 2018). In addition to real time weather information, Mesonet provides essential information through its suite of weather tools such as farm monitor, degree-day heat units, first hollow stem advisor, and, irrigation planner, among others, which have been developed with the ultimate goal of supporting agricultural management decisions. Overestimation of ET_{ref} will limit the ability to leverage the investments in weather monitoring infrastructure to improve agricultural water conservation in critical times in water-scarce irrigated areas. Accounting for station aridity effects creates an opportunity to improve the accuracy of the Mesonet ET_{ref} estimates and the effectiveness of its irrigation planner. This, in turn, can contribute to increasing the economic benefit of the weather-monitoring infrastructure in Oklahoma in terms of savings in pumping costs, while supporting water conservation to mitigate the overdraft of water in areas where irrigation decisions are made based on over-estimated ET_{ref}.

3.4. CONCLUSIONS

The Oklahoma Mesonet provides useful tools and information such as the daily ET_{ref} estimates to assist producers in irrigation decision making. However, station aridity effects associated with deviation of the surface conditions from reference surface induces a positive bias in the estimates

of ET_{ref}. Using MDD, RH_{max} and NDVI as indicators of station aridity, this study shows that the phenomenon is prevalent across the 83 Mesonet stations included in this analysis. The Mesonet stations located in western 30 counties of Oklahoma, where the majority of the state's irrigated areas are located, had a larger MDD, and a smaller RH_{max} and NDVI, indicating that they are more prone to station aridity effects compared with the rest of OK, especially in drier regions during droughts. The resulting overestimation of ET_{ref} can limit the ability of the Mesonet to provide accurate water requirement information to support irrigation decisions. The stations with the highest station aridity are located in Texas, Cimarron, and Caddo counties, which have the largest irrigated areas among all Oklahoma counties. A better understanding of the effects of station aridity and applying necessary adjustments to correct the positive bias in the ET_{ref} estimates can help improve the use of weather monitoring infrastructure for better agricultural water management.

CHAPTER IV

IMPROVING THE ESTIMATES OF REFERENCE EVAPOTRANSPIRATION IN THE OKLAHOMA MESONET

4.1. INTRODUCTION

The need for accurate reference evapotranspiration (ET_{ref}) estimates has been recognized by various stakeholders as it helps in quantifying amounts of water that enters groundwater aquifers (Huntington et al., 2016), managing the effects of climate change (Wilhite, 2000), basin water balance, irrigation systems design, improvements in crop yields and water use efficiency. With the expected impacts of station aridity on the quality of ET_{ref} estimates from OK Mesonet stations (see Chapter III), it is imperative to quantify potential inaccuracies and explore different methods to improve the accuracy of ET_{ref} estimates.

Penman Monteith (PM) method requires an ensemble of weather variables including solar radiation (Rs), wind speed at 2m height (W), relative humidity (RH) (or actual vapor pressure ea), and air temperature (T). The main challenge in estimating ET_{ref} using the PM method is that all these required weather variables are not available at many weather stations (Trajkovic & Kolakovic, 2009). Also, the quality of such weather variables may be questionable. For example – reliability of solar radiation (Llasat & Snyder, 1998), wind speed at 2m height (Jensen et al., 1997), and relative humidity (Allen, 1996) data is questioned in the past. The Oklahoma Mesonet, a world class network of weather stations, provides measurement of the required variables for the

PM method because of its high standards of Quality Assessment and Quality control (QAQC) process (Fiebrich et al., 2010; Shafer et al., 2000). It uses the standardized reference evapotranspiration (ET_{ref}) (ASCE, 2005) concept to estimate ET. Despite its quality assured data – Mesonet also suffers from station aridity because most of the stations do not have reference conditions inside the station boundary and in the surroundings. Station aridity occurs due to the lack of available water for the vegetation to be able to transpire. It directly affects T, RH, and W measurements. ASCE standardized PM method stresses on the importance of collecting weather data in well-watered agricultural settings so that the T and RH measurements are reflective of reference conditions.

In weather monitoring networks, T and RH sensors are installed at 1.5 to 3 m height above the ground for agricultural weather stations (Yoder et al., 2000) which sample the airstream from upwind of the stations. T and RH are most impacted by the ground surface conditions upwind of the stations. Ground surface conditions effect the energy partitioning and upwind airstream carries partitioned energy, either as latent heat flux (λ or ET) or sensible heat (H) towards the sensor. Allen (2006) called these upwind airstreams as the "artifacts" of surface energy exchanges. Studies have been carried out which make use of flux footprint models to assess the conditioning of T and RH measurements (Allen, 2006), impact of weather station siting (Kljun et al., 2004; Leclerc et al., 1997; Schuepp et al., 1990), and gauge the accuracy of upwind fetch (Gash, 1986; Schmid, 2002).

This chapter advances understanding of station aridity effects on ET_{ref} estimates at weather monitoring stations, offering insights to improve the ET_{ref} estimates. Our objectives are two-fold: (1) assess the implications of station aridity due to non-reference surface conditions for overestimation of ET_{ref} in agricultural areas, and (2) evaluate the performance of available correction methods to improve the ET_{ref} estimates. We present an in-depth analysis of station aridity at selected weather stations in the Oklahoma Mesonet based on the presence of reference

surface conditions or lack thereof during the period of peak crop growth. We examine the performance of four widely applied ET_{ref} correction methods by quantifying the difference in ET_{ref} estimates, accounting for surface conditions, irrigation applications in the surrounding environment, and wet and dry cycles. The paper contributes to weather-informed irrigation management by providing evidence about the need for and suitability of the available correction methods to improve ET_{ref} data from the Oklahoma Mesonet and other meso-scale weather monitoring networks that support irrigation decisions.

4.2. MATERIALS AND METHODS

4.2.1 DATASET

We use daily Mesonet dataset from 2000 – 2021. Hourly wind speed and direction (2 m) datasets were used to identify the primary wind directions for summer and fall seasons at the Mesonet stations. The variables include T_{max}, T_{min}, T_{dew}, and W_{avg}, and W_{dir}. Mesonet stations have a wide heterogeneity in the vegetative conditions in their surroundings which influence T and RH measurements (Fig 4.1). These stations are sited adhering to physical representativeness guidelines which states that a station should be representative of as large of area as possible. Therefore, the stations are located away from forests, lakes, and irrigated areas. Exception to this is the OSU/OU agricultural research stations such as Fort Cobb (FTCB) and Altus (ALTU) in southwestern OK. These stations too do not have standardized reference surface and are not irrigated but are located in the vicinity of agricultural areas. A station can be located over a surface with low vegetation but downwind of a vegetated field so that the sampled airstream from upwind direction is conditioned to reflect a reference environment (Jensen & Allen, 2016). Therefore, T and RH measurements and hence the estimated ET_{ref} at these stations should be closer to reference conditions when the upwind direction is from the vegetated fields. Example of Mesonet station siting is shown in Fig 1. Research stations such as Fort Cobb have agricultural

areas nearby. Hobart is located on an airstrip to provide information of the ambient weather at the airport. Cherokee is located in the outskirts of a town to provide ambient weather and forecast information relevant to the town.

Figure 4.1. Aerial imagery with wind rose for summer and fall seasons for 6 Mesonet stations. Images are 500 m on each side with concentric circles of radius 100m, 200 m, and 500m (inside out) respectively. Imagery created from Google Earth Pro.

Selection criteria to compare and adjust ET_{ref} –

We select the stations which resemble reference conditions and compare their estimated ET_{ref} with nearby stations with similar climatic conditions. The two sets of stations to compare are – Set 1 (Altus, Tipton, Mangum) and Set 2 (Fort Cobb, Apache, Hinton) (Fig 4.2). To demonstrate and quantify the effects of station aridity estimated ET_{ref} from the Mesonet – it must be established that the stations are similar except for the land surface conditions around them. The factors used to ascertain the similarity were location, elevation, and the aridity indicators i.e., MDD and RH_{max}. We investigated two sets of stations which are in the same southwest climate

division of Oklahoma (Fig 4.2). The stations in each of these sets have similar elevation – Altus (416 m), Tipton (387 m), Mangum (460 m) and Fort Cobb (422 m), Hinton (493 m), Apache (440 m). The stations will resemble reference conditions during the periods when the crops are at effective full cover and the sensors at these stations receive ET fluxes when the upwind direction is from these nearby agricultural fields.

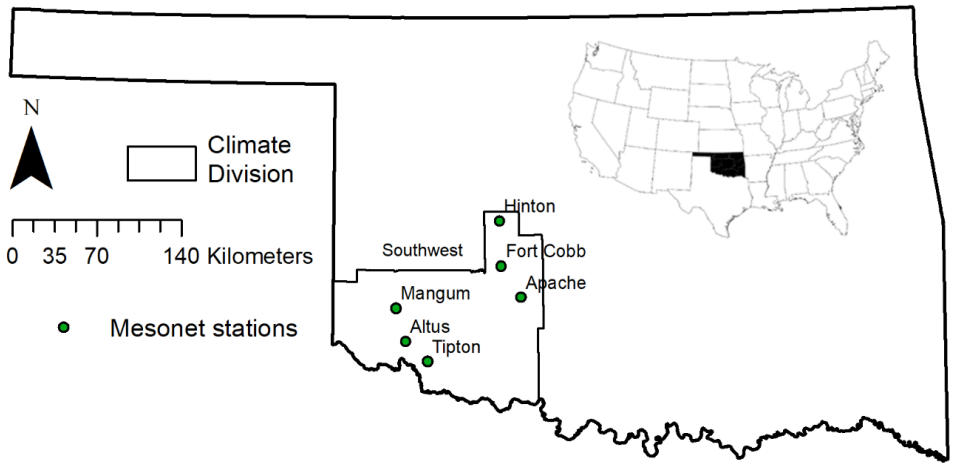

Figure 4.2. Location of Oklahoma Mesonet stations used in this study.

Normalized difference vegetation index (NDVI) was used to examine the vegetation in and around the Mesonet station because it has a strong correlation with green biomass and serves as an indicator of crop growth and monitoring (Esquerdo et al., 2011; Ji-Hua & Bing-Fang, 2008; Rangoonwala et al., 1993; Yang et al., 2011; Zhang et al., 2014). Reference condition periods were selected based on the NDVI of the surrounding fields taking into consideration the primary wind direction. NDVI is a necessary but not sufficient condition for reference conditions to exist (Blankenau et al., 2020). But still it was used a criterion to identify reference conditions around the stations. It can be calculated as –

$$NDVI = \frac{NIR - RED}{NIR + RED} \qquad \text{Eq 1}$$

where, NIR = reflectance in the near-infrared band and RED = reflectance in the visible red band.

We used Landsat and Sentinal imagery and derive the NDVI images using EOS Landviewer to identify those periods in which crops in the nearby agricultural fields are in the effective full cover growth stage. It is assumed that when NDVI ≥ 0.7 – the crops are at effective full cover. Using the daily dataset from the pair of reference and non-reference Mesonet stations we compare the ET_{ref} for the selected periods to assess the effects of station aridity on the estimates of ET_{ref}. In this study we used ET_{ref} and ET_o interchangeably as both represent the same thing. Because of the availability of high-resolution images – the imagery in and after 2015 was selected to compare the periods. It is important to highlight the fact that even the irrigated stations do not have agriculture surrounding them in the years when there is a shortage of water. These stations are actively managed because they are used for agricultural research.

Altus station in Set 1 is reference during the selected periods, Tipton is non reference as it has bare soil in the prominent wind direction (south), and Mangum is located on natural vegetation in rangeland. In Set 2 Fort Cobb has irrigated agricultural strip in the prominent wind direction i.e., south while Apache and Hinton are located on natural vegetation in rangeland whose surroundings are not managed. The periods chosen for the comparison using NDVI ≥ 0.7 are in Table 1. Fig 4.3 provides an example of the NDVI in the station surroundings in the selected periods.

Table 4.1. Start and End dates for effective full cover of crops in the station surroundings

Year	Start Altus	End Altus	Start Fort Cobb	End Fort Cobb
2015	X	X	X	X
2016	06/08	08/10	X	X
2017	16/08	11/10	X	X
2018	27/08	20/09	04/08	23/08
2019	16/08	25/09	28/08	08/09
2020	31/07	25/08	X	X
2021	28/07	06/09	28/07	06/09

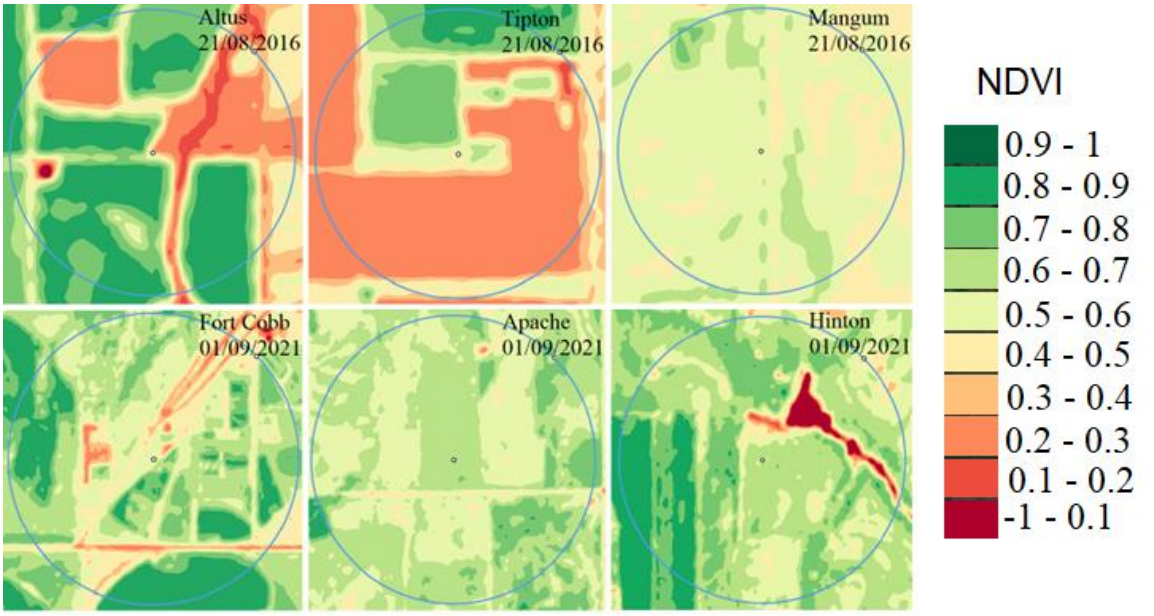

Figure 4.3. NDVI of the two sets of Mesonet stations in the selected periods. Stations are located at the center of circles which are 500 m in radius. Imagery obtained from EOS Landviewer.

To demonstrate that the selected stations are similar except for the land surface conditions around them we selected the periods during which the land surface conditions are functionally similar so that the estimated ET_{ref} from the three stations in a set is close to one another. Rainy days are the periods during which crops, natural vegetation, and bare soil receive enough water so that both vegetation and top layer of bare soil can transpire and evaporate water respectively from the surface. During such periods the stations will resemble reference conditions. We selected days with > 2.5 mm rainfall during the selected periods and compared their MDD and RH_{max}. MDD values < 2 °C and RH_{max} values > 80% during growing season period when it is warmer are good indicators that reference conditions existed.

4.2.2. METHODS TO IMPROVE THE ESTIMATES OF ET_{ref}

The various methods to improve the estimates of ET_{ref} in weather stations which do not have reference conditions around them mainly based on adjusting temperature and humidity data. The

adjustments are done so that the data obtained from non-reference sites resemble reference conditions. FAO 56 and ASCE proposed methods to adjust daily or monthly data are –

1. Estimation of T_{dew} using T_{min} (FAO-56, Method 1) - It is done by –

$$T_{dew} = T_{min} - K_0 \quad \text{Eq 2}$$

where, K_0 = 0 °C is recommended for humid to sub humid environments.

2. Estimation of T_{dew} using T_{min} (FAO-56 Method 2) - It is done by –

$$T_{dew} = T_{min} - K_0 \quad \text{Eq 3}$$

where, K_0 = 2 °C is recommended for arid to semi-arid environments.

3. Adjusting T_{max}, T_{min}, and T_{dew} to reflect reference environments (FAO-56, Method 3) – When K_0 is based on constant, according to FAO-56 (Allen et al., 1998) temperatures can be corrected for each month or day as

$$(T_{max})_{cor} = (T_{max})_{obs} - (\frac{\Delta T - K_0}{2}) \quad \text{Eq 4}$$

$$(T_{min})_{cor} = (T_{min})_{obs} - (\frac{\Delta T - K_0}{2}) \quad \text{Eq 5}$$

$$(T_{dew})_{cor} = (T_{dew})_{obs} - (\frac{\Delta T - K_0}{2}) \quad \text{Eq 6}$$

for $\Delta T > K_0$, where cor refers to corrected and obs to observed values. K_0 is a constant equal to 2° C when non reference station is not compared to a reference station. It must be ensured that $(T_{min})_{cor} > (T_{dew})_{cor}$. Estimate the ETref using the corrected values of temperatures.

4. NDVI based method to adjust T_{max} and T_{min} (Method 4) – We used Sentinel and Landsat imagery from 2016 to 2021 to calculate NDVI around each selected station. Following Blankenau et al. (2020), average NDVI for a station was computed as the average NDVI over areas within 500 m and 2 km radii of each station to account for the influence of local and regional scale aridity on the fluxes received by the sensor.

Aridity rating was computed for each selected period using the following equations –

a. If NDVI < 0.15: Aridity Rating (AR) = 1
b. If 0.15 < NDVI < 0.70:

$$AR = \frac{0.70 - NDVI}{0.70 - 0.15} \quad \text{Eq 7}$$

c. If NDVI ≥ 0.70: AR = 0

Values of T_{max} and T_{min} were reduced by the amount = Aridity Rating × Values of temperature in table below.

Table 4.2. Mean monthly departure of air temperatures between irrigated and non-irrigated site (Allen 1982)

Month	Mar	Apr	May	Jun	Jul	Aug	Sep	Oct
Aridity Adjustment (°C)	0	1	1.5	2	3.5	4.5	3	0

ET_o was computed using the adjusted values of T_{max} and T_{min} using the PM equation. This method of adjusting ET_o had originated from Allen (1982) in which they used average monthly departures of T between arid and irrigated sites in southern Idaho. Information regarding sites was obtained through questionnaire and telephonic conversations. An aridity rating was then given to each station based on the information received about site conditions. In this study we instead used NDVI to calculate the aridity rating. We apply the corrections in non reference stations on the days when MDD > 2 °C.

4.3. RESULTS AND DISCUSSION

4.3.1. Similarity between stations

We found 22 days in set 1 and 5 days in set 2 when all the three stations received rainfall > 2.5 mm. We observed an average MDD and RH_{max} of -1.04 °C and 99 %, -0.71 °C and 98%, and -1.28 °C and 99%, in Altus, Tipton, and Mangum stations, respectively. The average values of MDD and

RH_{max} for set 2 stations were -0.60 °C and 96%, -0.61 °C and 97%, and -0.53 °C and 97%, respectively for Fort Cobb, Hinton, and Apache. During these rainy days the average ET_o difference between Tipton and Altus was 0.41 mm and between Apache and Altus was 0.09 mm. Similarly, the average differences in ET_o between Apache and Fort Cobb was -0.07 mm, and between Hinton and Fort Cobb was 0.39 mm. The observed smaller values of MDD, greater RH_{max}, and smaller ET_o differences between the stations during rainy days suggest that the three stations in each of the sets were similar to each other. The similarity can be attributed to the similar behavior of the land surface conditions for the purpose of estimation of ET_o during rain events when station aridity effects are negligible. By contrast, the different land surface conditions in and around the stations cause varying levels of station aridity during dry days, resulting in differences in the ET_o (see section 4.3.2).

4.3.2. Comparison of Mesonet estimated ET_o

On comparing the ET_o estimates (Fig 3) we found that Altus ET_o was smaller than ET_o at Tipton station 69.68% of the time during the analysis period. Altus ET_o was also smaller than Mangum station 23.23% of the time. Fort Cobb had a smaller ET_o than Apache station 50.68% of time, and Hinton station 78.20 % of the time. The mean difference was 0.59 mm, -0.25 mm, 0.16 mm, and 0.50 mm between Tipton-Altus, Mangum-Altus, Apache-Fort Cobb, and Hinton-Fort Cobb, respectively. The smaller ET_o of Altus than Tipton is expected. Unlike Tipton the land south of Altus has agricultural crops during the selected periods. Therefore, the sensors mounted at Altus station should receive latent heat fluxes from transpiring crops while sensors at Tipton station receive sensible heat from the bare patch of land. Mangum had a smaller ET_o most of the time than Altus which is likely due to the presence of natural vegetation in the surroundings which means that there would be enough moisture present in the air to bring observations of T and RH at Mangum closer to reference conditions. Therefore, although irrigated areas do not exist around

Mangum station, the location of this station over natural vegetation that are not actively altered by human activity allows its use as a benchmark for ET_o estimation.

Greater differences between the ET_o of Altus and Tipton were observed on dry days when there was no rainfall. For example, on 27/08/2018 and 28/08/2018 (Fig. 4.4.) the differences in the estimated ET_o were 3.04 mm between Altus and Tipton. Similarly, the difference between Fort Cobb and Apache on 4/08/2018 was 2.24 mm. The sharp drops in the ET_o were due to the rain clouds which reduced the incoming solar radiation and possibly because of the drops in temperature. ET_o of all the three stations during the rainfall days in both sets was almost equal because of equilibrium conditions. After a rainfall event the bare patch of soil becomes wet and can provide water for evaporation. During these periods the lower layer of air becomes saturated with water. Therefore, during these periods the ET_o estimated at a station located on patch of bare soil will almost be equal to that obtained from reference station given all other variables are equal. As the cloud cover decreases and the sky starts to clear up the ET_o also increases. During these periods bare soil starts to dry up and we see increasing difference in the ET_o of reference and non-reference stations. An example of such behavior is the period after 15/09/2018 upto 19/09/2018 where we see gradually increasing differences in the estimated ET_o of Altus and Tipton. Similarly, in the period between 30/08/2019 and 8/09/2019 we can observe increasing differences between Fort Cobb, Apache, and Hinton.

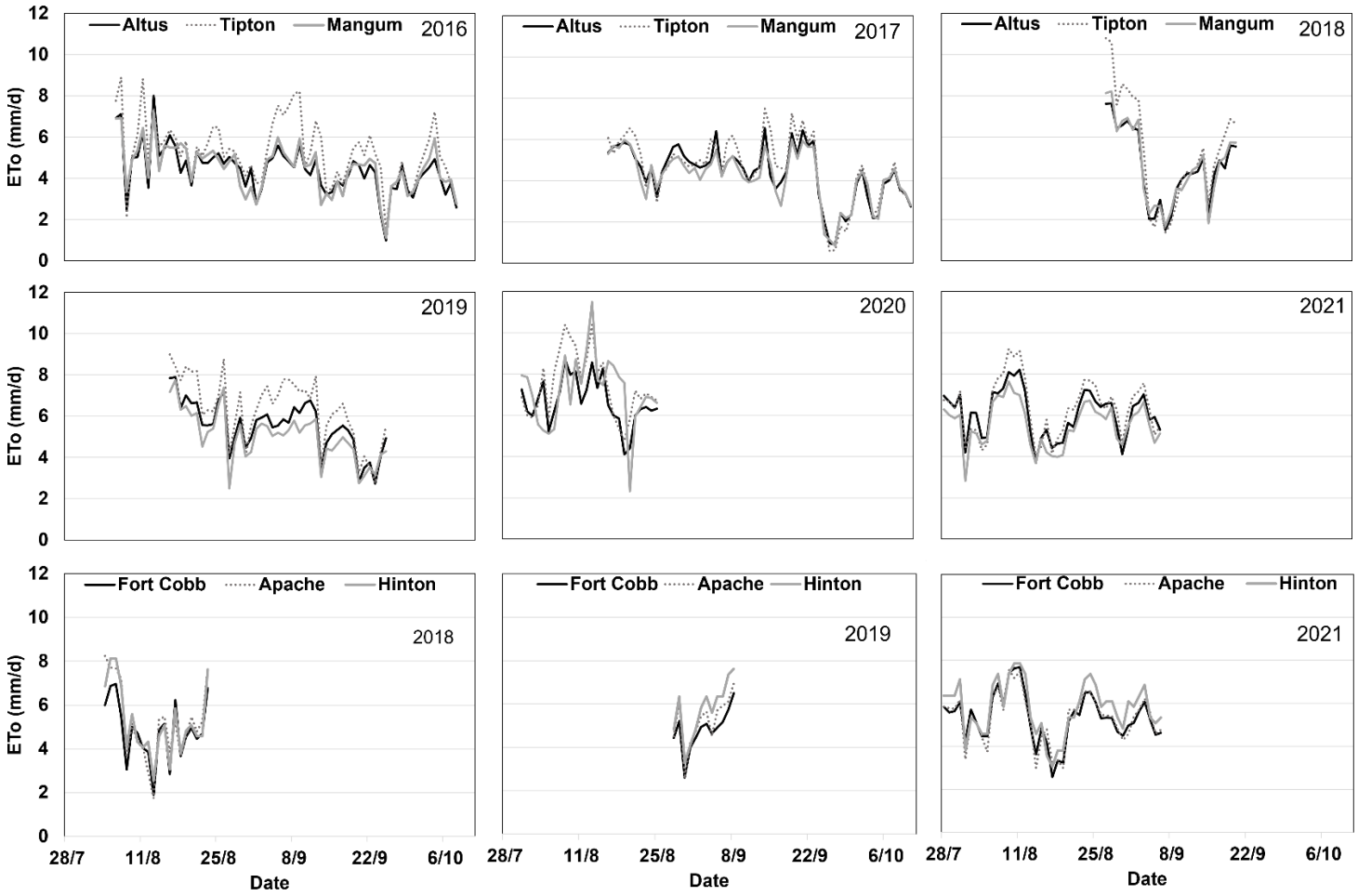

Fig. 4.4. Comparison of estimated ET_o of nearby Mesonet stations for selected periods

4.3.3. COMPARING MDD AMONG STATIONS

MDD serves as an indicator of the magnitude of station aridity (Table 4.3). Daily average MDD for the seasons (summer, fall and growing) is greater than annual (2000-2021) averages for all the six stations. This is because annual average includes winter seasons during which the temperatures are very low, which brings the overall average lower than seasonal averages. During summer & fall and growing season we observe MDD > 2 °C in Altus and Ford Cobb stations which have been selected as reference stations. The reason behind this is that these two stations are agricultural research stations, and the managers grow crops in their vicinity only when there is sufficient water available to support the growth of crops. Therefore, during drought years when water is limited, they do not grow crops and the land in their south remains bare which leads to greater values of MDD. It is to be noted that Altus always had average MDD greater than Mangum. A possible reason for such behavior could be that the mangers at Altus consistently trim the grass (natural vegetation) inside the station boundary therefore during low and calm wind conditions the sensors receive the sensible heat flux originating just below the tower impacting the daily MDD values.

Table 4.3. Average MDD of the paired stations for different time periods

Period/Station	Altus	Tipton	Mangum	Fort Cobb	Apache	Hinton
2000 - 2021	1.92	1.53	0.51	2.63	1.10	1.16
Summer & Fall	2.43	2.56	1.03	4.41	1.56	1.64
Growing Season	2.39	2.44	1.07	3.95	1.41	1.50
2016 SP	-0.47	1.19	-0.87	X	X	X
2017 SP	0.24	0.66	-0.88	X	X	X
2018 SP	0.72	1.74	-0.15	0.08	0.80	0.62
2019 SP	1.42	2.43	0.39	-0.41	0.51	0.82
2020 SP	0.90	3.65	0.70	X	X	X
2021 SP	1.92	1.95	-0.09	0.12	0.01	1.37

4.3.4. ADJUSTING THE ET_o

Adjustments were applied on the temperatures of Tipton, Mangum, Apache and Hinton, using the four methods only during the days in which MDD > 2 °C in the selected periods (Table 4.4). The largest reduction in the ET_o between Tipton and Altus was observed after the application of Method 4 which resulted in average ET_o difference in the whole selected period between the stations to be below zero. After Method 4 (M4), Method 1 (M1) had the best performance in terms of the average ET_o and maximum ET_o difference followed by Method 2 (M2) and Method 3 (M3). Between Mangum and Altus stations there were negative average ET_o difference because during most of the selected period Mangum had equal or smaller ET_o than Altus. This corroborates that stations located over natural vegetation can also resemble reference condition and can be used to estimate ET_o with good accuracy. Since the average ET_o difference of Mangum is less than that of Altus and also the MDD of Mangum is less than that of Altus, the ET_o does not require to be corrected for station aridity. However, further studies should be carried out during drought years to observe and analyze the effects of station aridity on estimated ET_o and MDD of Mangum since it is located on natural vegetation which depends on water supplied by rainfall.

The performance of M4 was best in terms of reducing the average ET_o difference between Apache and Fort Cobb followed by M1, M2, and M3 respectively. Similarly for Hinton and Fort Cobb M4 performed the best followed by M2, M1, and M3. M3 was the most conservative in adjusting the temperatures while the NDVI based on M4 reduced T_{max} and T_{max} more than any other method resulting in the largest decrease in the ET_o values. Negative minimum ET_o difference between the stations indicate that there were periods when ET_o of non-reference station were less than that of reference station. These were the periods of rainfall when the stations did not experience the aridity effects. This phenomenon can be observed in both sets of stations.

Table 4.4. Differences in adjusted ET_o between non reference and reference stations

Adjustment	Descriptive Statistics	Set 1 ET_o (mm)		Set 2 ET_o (mm)	
		Tipton – Altus	Mangum – Altus	Apache - Fort Cobb	Hinton - Fort Cobb
Before adjustment	Maximum	3.05	0.76	2.24	1.64
	Minimum	-0.76	-1.52	-0.98	-0.61
	Average	0.59	-0.24	0.16	0.50
Method 1 (M1)	Maximum	2.54	0.76	1.06	1.27
	Minimum	-1.47	-1.83	-1.10	-1.32
	Average	0.10	-0.28	-0.01	0.28
Method 2 (M2)	Maximum	2.54	0.76	1.34	1.27
	Minimum	-1.01	-1.52	-1.10	-0.76
	Average	0.40	-0.26	0.04	0.36
Method 3 (M3)	Maximum	2.54	0.76	1.36	1.36
	Minimum	-0.82	-1.52	-0.93	-0.76
	Average	0.49	-0.25	0.15	0.39
Method 4 (M4)	Maximum	2.54	0.76	1.38	1.37
	Minimum	-1.25	-4.31	-1.10	-0.76
	Average	-0.32	-0.59	0.02	0.36

In general, all of these methods work on adjusting the air and dew point temperatures in proportion to the station aridity. In M1, M2, and M3 the station aridity is based on the MDD at the stations. In M1, T_{dew} is replaced by T_{min} without using any K_0 while in M2 T_{dew} is replaced by $T_{min} – K_o$ (= 2 °C) and hence the estimated T_{dew} in M1 is greater than T_{dew} estimated in M2. Therefore, the ET_o estimated using M1 is lesser than that in M2. In M3, we reduce $T_{max,}$ T_{min}, and T_{dew} only by a small amount as we subtract K_0 (= 2 °C) from the MDD and reduce it by half. So essentially, we reduced both T_{max} and T_{min} by equal amounts which reduces the estimated ET_o while we also reduced T_{dew} which increases the estimated ET_o. Therefore, the overall reduction in the ET_o is less than the reduction in the estimated ET_o after the application of M1 and M2. This is why we observe least average differences in ET_o of reference and on reference stations after the application of M1 followed by M2 and M3. Since the adjusted T_{dew} using T_{min} of a non-reference station became closest to the T_{dew} of reference station using M1 but never went below it – using the results of this study it is recommended to use method M1 for stations in southwestern OK.

Using the first three methods, in no case we observed the ET_o of the non-reference stations to be reduced below the ET_o of reference stations. In M4 the air temperature adjustments are based on the station aridity rating developed by using NDVI of the station surroundings. M4 reduced both T_{max} and T_{min} such that in one case the average ET_o of non-reference station (in the case of Tipton) became less than the average ET_o of reference stations (Altus). This is because the AR obtained by NDVI is multiplied the monthly air temperature departure values observed in southern Idaho (Allen 1982) which may be more than those observed between a reference station and a non-reference station in southwest OK leading to greater reductions in air temperatures than required. It is advised to develop regional mean monthly air temperature departure values before applying the NDVI based M4 method.

4.4. CONCLUSIONS

This study compared the PM estimated ET_o for two sets of stations which are – Set 1: Altus, Tipton, and Hinton and Set 2: Fort Cobb, Apache, and Hinton. Both of these sets of stations are located in the southwest climate division of Oklahoma. It was observed that Tipton had a greater ET_o than Altus which was greater than 2 mm/day on some days. The possible reason is because the land south of Tipton had no vegetation at all during the selected period. ET_o of Mangum generally was below than that of Altus because of the presence of natural vegetation inside the station boundary and in the surroundings. Apache and Fort Cobb had little differences in the estimated ET_o which averaged at 0.16 mm during the selected period. In both sets of stations, estimated ET_o between reference and non-reference stations become closer during the rainy periods and start to increase as the water becomes limited for the natural vegetation. In this research we observed that the station which had undisturbed natural vegetation surrounding it has a similar response as the station which had agricultural area in the vicinity in its primary wind direction. A comparison of weather datasets and ET_o of the selected pair of stations should be

made with actual reference stations in the area to fully understand the differences in the climatic observations made by the sensors as it pertains to land surface conditions.

This study also analyzed the performance of different methods to adjust air temperatures to reflect reference environments in stations which are subjected to station aridity. NDVI based method reduced the greatest amount from air temperatures and hence the ET_o. Method 1 performed better than others in reducing the ET_o because K_0 is kept at 0 °C, which should be the case for semi humid climates which exist in southwest climate division of Oklahoma. The methods can increase the ET_o on wet days because on such days T_{min} is likely to be less than T_{dew} and if we replace T_{dew} by T_{min} it will bring T_{dew} down and will increase the ET_o. This why we applied the corrections on the days in which MDD > 2 °C. Therefore, caution should be exercised while using the adjustment procedures on days when MDD thresholds are not crossed in the Oklahoma Mesonet.

CHAPTER V

SUMMARY AND CONCLUSION

5.1. SUMMARY

Agriculture in Oklahoma is heavily dependent on natural surface and groundwater resources especially in the western climate divisions. Historical trends in air temperature and precipitation show increasing trends consistent with the existing literature in the Great Plains region of the US. ET_o show decreasing trends in summer season which could possibly be because of the evaporative cooling due to increased agriculture in the region. We observed drought patterns similar to the 1950's in the past decade (2010's).

These trends are likely to increase the station aridity in the Oklahoma Mesonet stations which are not surrounded by irrigated agriculture. Droughts will limit the water supply to natural vegetation which will cause overestimation of ET_o. We observed greater values of station aridity during such drought periods with the help of RH_{max}, MDD, and NDVI indicators. For example, RH_{max} frequently dropped below 80%, MDD went as much as 12 °C, and NDVI dropped below 0.4 in most of the western Mesonet stations during the summer of 2011.

During the dry periods we observed ET_o differences of more than 2 mm/day between the Mesonet stations which had irrigated agriculture surrounding them and which had bare soil nearby in the upwind direction. The stations which had natural vegetation inside and, in the surroundings, can

be used to estimate ET_o using the PM method. However, the performance of such stations remains to be seen during the droughts. The ET_o of such non reference stations was adjusted using the recommended and new NDVI based methods. All the methods reduced the estimated ET_o by reducing the observed air temperatures at the stations. However, it is important to exercise caution while applying these adjustment methods on the days in which it rains or MDD does not exceed the thresholds.

5.2. CONCLUSIONS AND FUTURE WORK

The observed trends in chapter 2 indicate that increasing temperature trends are likely going to increase evaporation losses from surface water resources and with declining groundwater levels such as in Ogalalla aquifer in panhandle – water will be the limiting factor in crop productivity across the state. Agriculture will be vulnerable to droughts with recurring drought patterns in the state. Examples include drying of lake Altus and Fort Cobb reservoir during the summer of 2011. Increases in temperatures and rainfall may also affect water supply, hydroelectricity, irrigation, and ranching. Increasing precipitation trends may cause flash flooding, which may cause erosion and may result in nutrient and crop loss and damage to property, or even loss of life. The research will help guide water managers in adapting to sustain agricultural water availability and production.

In the Oklahoma Mesonet station aridity affects the estimation of ET_{ref} and hence the various tools it provides to help farmers plan irrigation scheduling. The indicators (I_{RH}, I_{MDD}, and I_{NDVI}) used in this study demonstrate that western Oklahoma which has most of the irrigated agriculture in the state is more susceptible to station aridity. The stations in the western climate divisions do not have the required surface conditions to accurately estimate ET_{ref}. The indicators were highly correlated with precipitation and elevation. The stations with largest station aridity such as Kenton, Boise city, Cheyenne, and Medicine Park which are located in counties where agriculture

highly depends on natural water resources as it is limited by water supplied through rainfall. The research helps us to analyze surface aridity using the indicators which can be used to develop the K_o values for individual stations to access its magnitude and amount of correction required in air and dew point temperatures so that the dataset from these stations can resemble reference conditions. This provides us with an opportunity to improve the estimation of ET_o in western OK.

In southwestern OK we compared Mesonet estimated ET_o at stations located over reference, non-reference, and natural vegetation to observe over 2mm/day overestimation. We adjusted these overestimations with the help of four methods to improve the estimations. Replacing T_{dew} with T_{min} seemed to work better than the other methods. NDVI based method can be improved by developing K_o values for the individual stations. The results of this study can help improve the use of weather monitoring infrastructure for better agricultural water management.

Future research can address the question of historical climatic trends on smaller spatial scales such as daily or hourly to provide insights into the trends in extreme temperature, rainfall, and ET_{ref}. Understanding of the effects of station aridity on estimated ET_{ref} and MDD at stations located in areas surrounded by natural vegetation can be advanced by further studies carried out during drought years to determine the effects of reduced rainfall. The NDVI-based method for correcting ET_{ref} requires more scrutiny and development of regional mean monthly air temperature departure values to quantify the required adjustments.

REFERENCES

Abtew, W., & Melesse, A. (2013). Climate Change and Evapotranspiration. In *Evaporation and Evapotranspiration: Measurements and Estimations* (pp. 197-202). Springer Netherlands. https://doi.org/10.1007/978-94-007-4737-1_13

ASCE. (2005). *The ASCE standardized reference evapotranspiration equation. Technical Committee on Standardization of Reference Evapotranspiration.* *https://ascelibrary.org/doi/book/10.1061/9780784408056*. American Society of Civil Engineers.

Babst, F., Bouriaud, O., Poulter, B., Trouet, V., Girardin, M. P., & Frank, D. C. (2019). Twentieth century redistribution in climatic drivers of global tree growth. *Science Advances*, *5*(1), eaat4313.

Bates, B., Kundzewicz, Z., & Wu, S. (2008). *Climate change and water*. Intergovernmental Panel on Climate Change Secretariat.

Brock, F. V., Crawford, K. C., Elliott, R. L., Cuperus, G. W., Stadler, S. J., Johnson, H. L., & Eilts, M. D. (1995). The Oklahoma Mesonet: a technical overview. *Journal of Atmospheric and Oceanic Technology*, *12*(1), 5-19.

Broner, I. (1989). *Irrigation scheduling* Colorado State University. Libraries.

Brown, M., Antle, J., Backlund, P., Carr, E., Easterling, B., Walsh, M., ... & Tebaldi, C. (2015). Climate change, global food security and the US food system.

Calanca, P., Roesch, A., Jasper, K., & Wild, M. (2006). Global warming and the summertime evapotranspiration regime of the Alpine region. *Climatic Change*, *79*(1), 65-78.

Condon, L. E., Atchley, A. L., & Maxwell, R. M. (2020). Evapotranspiration depletes groundwater under warming over the contiguous United States. *Nature communications*, *11*(1), 1-8.

Cong, Z., Yang, D., & Lei, Z. (2008). Did evaporation paradox disappear after the 1980s? A case study for China. *Geophysical Research Abstracts. EGU, Munich, Germany*

Gaertner, B. A., Zegre, N., Warner, T., Fernandez, R., He, Y., & Merriam, E. R. (2019). Climate, forest growing season, and evapotranspiration changes in the central Appalachian Mountains, USA. *Science of the Total Environment*, *650*, 1371-1381.

Gleick, P. H. (1993). *Water in crisis* (Vol. 100). New York: Oxford University Press

Groffman, P., Kareiva, P., Carter, S., Grimm, N., Lawler, J., Mack, M., Matzek, V., & Tallis, H. (2014). Ch. 8: Ecosystems, biodiversity, and ecosystem services. *Climate change impacts in the United States: The third national climate assessment*, *841*, 195-219.

Kukal, M. S., & Irmak, S. (2018). Climate-driven crop yield and yield variability and climate change impacts on the US Great Plains agricultural production. *Scientific Reports*, *8*(1), 1-18.

Masson-Delmotte, V., Zhai, P., Pirani, A., Connors, S. L., Péan, C., Berger, S., ... & Zhou, B. (2021). Climate change 2021: the physical science basis. *Contribution of working group I to the sixth assessment report of the intergovernmental panel on climate change*, 2.

Melillo, J. M., Richmond, T., & Yohe, G. (2014). Climate change impacts in the United States. *Third national climate assessment*, *52*.

Piao, S., Nan, H., Huntingford, C., Ciais, P., Friedlingstein, P., Sitch, S., Peng, S., Ahlström, A., Canadell, J. G., & Cong, N. (2014). Evidence for a weakening relationship between interannual temperature variability and northern vegetation activity. *Nature communications*, *5*(1), 1-7.

Rungee, J., Bales, R., & Goulden, M. (2019). Evapotranspiration response to multiyear dry periods in the semiarid western United States. *Hydrological Processes*, *33*(2), 182-194.

Seager, R., Lis, N., Feldman, J., Ting, M., Williams, A. P., Nakamura, J., Liu, H., & Henderson, N. (2018). Whither the 100th Meridian? The once and future physical and human geography of America's arid–humid divide. Part I: The story so far. *Earth Interactions*, *22*(5), 1-22.

Shafer, M., Ojima, D., Antle, J. M., Kluck, D., McPherson, R. A., Petersen, S., Scanlon, B., & Sherman, K. (2014). Ch. 19: great plains. *Climate change impacts in the United States: The third national climate assessment*, 441-461.

Shideler, D. (2015). Contribution of Agriculture to Oklahoma's Economy: 2015. In: Oklahoma State Univ.

Taghvaeian, S. (2014). Irrigated Agriculture in Oklahoma. *Oklahoma Cooperative Extension, Publication BAE-1530*.

Trenberth, K. E. (2005). The impact of climate change and variability on heavy precipitation, floods, and droughts. *Encyclopedia of hydrological sciences*, *17*.

Vadeboncoeur, M. A., Green, M. B., Asbjornsen, H., Campbell, J. L., Adams, M. B., Boyer, E. W., Burns, D. A., Fernandez, I. J., Mitchell, M. J., & Shanley, J. B. (2018). Systematic variation in evapotranspiration trends and drivers across the Northeastern United States. *Hydrological Processes*, *32*(23), 3547-3560.

von Braun, J. (2020). Climate Change Risks for Agriculture, Health, and Nutrition. In W. K. Al-Delaimy, V. Ramanathan, & M. Sánchez Sorondo (Eds.), *Health of People, Health of Planet and Our Responsibility: Climate Change, Air Pollution and Health* (pp. 135-148). Springer International Publishing. https://doi.org/10.1007/978-3-030-31125-4_11

Vose, R. S., Applequist, S., Squires, M., Durre, I., Menne, M. J., Williams Jr, C. N., Fenimore, C., Gleason, K., & Arndt, D. (2014). Improved historical temperature and precipitation time series for US climate divisions. *Journal of Applied Meteorology and Climatology*, *53*(5), 1232-1251.

Walthall, C. L., Anderson, C. J., Baumgard, L. H., Takle, E., & Wright-Morton, L. (2013). Climate change and agriculture in the United States: Effects and adaptation.

Watson, R. T., Zinyowera, M. C., & Moss, R. H. (1996). *Climate change 1995. Impacts, adaptations and mitigation of climate change: scientific-technical analyses*.

Zhang, M., Geng, S., Ransom, M., & Ustin, S. (1996). The effects of global warming on evapotranspiration and alfalfa production in California. *Department of Land, Air and Water Resources, University of California, Davis*.

Almas, L. K., Colette, W. A., & Adusumilli, N. C. (2008). Economic value of groundwater resources and irrigated agriculture in the Oklahoma Panhandle. Retrieved from

Anwar, M. R., Liu, D. L., Macadam, I., & Kelly, G. (2013). Adapting agriculture to climate change: a review. Theoretical and applied climatology, 113(1), 225-245. doi:10.1007/s00704-012-0780-1

Balcombe, C. (2014). Upper Red River Basin Study. U.S. Department of the Interior - Bureau of Reclamation. Retrieved from https://www.usbr.gov/watersmart/bsp/docs/fy2014/UpperRedRiverBasinStudy.pdf

Bartush, K. B., Banner, J., Brown, D., Lemery, J., Lin, X., Loeffler, C., . . . Ziolkowska, J. (2018). Southern Great Plains - In Impacts, Risks, and Adaptation in the United States. Fourth National Climate Assessment, II, 987–1035.

Benestad, R. (2013). Association between trends in daily rainfall percentiles and the global mean temperature. Journal of Geophysical Research: Atmospheres, 118(19), 10,802-810,810.

Capparelli, V., Franzke, C., Vecchio, A., Freeman, M. P., Watkins, N. W., & Carbone, V. (2013). A spatiotemporal analysis of US station temperature trends over the last century. Journal of Geophysical Research: Atmospheres, 118(14), 7427-7434.

Chauhan, B. S., Mahajan, G., Randhawa, R. K., Singh, H., & Kang, M. S. (2014). Global warming and its possible impact on agriculture in India. Advances in agronomy, 123, 65-121.

Dabanlı, İ., Şen, Z., Yeleğen, M. Ö., Şişman, E., Selek, B., & Güçlü, Y. S. (2016). Trend Assessment by the Innovative-Şen Method. Water Resources Management, 30(14), 5193-5203. doi:10.1007/s11269-016-1478-4

Dahl, N., & Xue, M. (2016). Prediction of the 14 June 2010 Oklahoma City extreme precipitation and flooding event in a multiphysics multi-initial-conditions storm-scale ensemble forecasting system. Weather and Forecasting, 31(4), 1215-1246.

Dawadi, S., & Ahmad, S. (2013). Evaluating the impact of demand-side management on water resources under changing climatic conditions and increasing population. Journal of Environmental Management, 114, 261-275.

Dos Santos, C. A., Neale, C. M., Mekonnen, M. M., Gonçalves, I. Z., de Oliveira, G., Ruiz-Alvarez, O., . . . Rowe, C. M. (2022). Trends of extreme air temperature and precipitation and their impact on corn and soybean yields in Nebraska, USA. Theoretical and applied climatology, 147(3), 1379-1399.

Easterling, D. R., Horton, B., Jones, P. D., Peterson, T. C., Karl, T. R., Parker, D. E., . . . Jamason, P. (1997). Maximum and minimum temperature trends for the globe. Science, 277(5324), 364-367.

Garbrecht, J. D., & Rossel, F. E. (2002). Decade-scale precipitation increase in Great Plains at end of 20 th century. Journal of Hydrologic Engineering, 7(1), 64-75.

Gilbert, R. O. (1987). Statistical methods for environmental pollution monitoring: John Wiley & Sons.

Gobiet, A., Kotlarski, S., Beniston, M., Heinrich, G., Rajczak, J., & Stoffel, M. (2014). 21st century climate change in the European Alps—A review. Science of the Total Environment, 493, 1138-1151.

Haan, C. T. (1977). Statistical methods in hydrology: Ames. IA: University, Press/Ames.

Hamed, K. H., & Rao, A. R. (1998). A modified Mann-Kendall trend test for autocorrelated data. Journal of hydrology, 204(1-4), 182-196.

Hargreaves, G. H., & Samani, Z. A. (1985). Reference crop evapotranspiration from temperature. Applied Engineering in Agriculture, 1(2), 96-99.

Higgins, R., Kousky, V., & Xie, P. (2011). Extreme precipitation events in the south-central United States during May and June 2010: Historical perspective, role of ENSO, and trends. Journal of Hydrometeorology, 12(5), 1056-1070.

Huntington, T. G. (2006). Evidence for intensification of the global water cycle: Review and synthesis. Journal of hydrology, 319(1-4), 83-95.

Hurrell, J. (2017). NATIONAL CENTER FOR ATMOSPHERIC RESEARCH STAFF (eds.), Last modified 07 Nov 2017. The Climate Data Guide: Hurrell North Atlantic Oscillation (NAO) Index (station-based).

Illston, B. G., Basara, J. B., & Crawford, K. C. (2004). Seasonal to interannual variations of soil moisture measured in Oklahoma. International Journal of Climatology: A Journal of the Royal Meteorological Society, 24(15), 1883-1896.

Irmak, S., Kabenge, I., Skaggs, K. E., & Mutiibwa, D. (2012). Trend and magnitude of changes in climate variables and reference evapotranspiration over 116-yr period in the Platte River Basin, central Nebraska–USA. Journal of hydrology, 420, 228-244.

Jain, S. K., & Kumar, V. (2012). Trend analysis of rainfall and temperature data for India. Current Science, 37-49.

Kendall, M. (1975). Rank correlation methods. 2nd impression. Charles Griffin and Company Ltd. London and High Wycombe.

Khand, K., Taghvaeian, S., & Ajaz, A. (2017). Drought and its impact on agricultural water resources in Oklahoma.

Kleinbaum, D.G., Kupper, L.L., Nizam, A. and Rosenberg, E.S., 2013. Applied regression analysis and other multivariable methods. Cengage Learning.

Kukal, M., & Irmak, S. (2016). Long-term patterns of air temperatures, daily temperature range, precipitation, grass-reference evapotranspiration and aridity index in the USA Great Plains: Part I. Spatial trends. Journal of hydrology, 542, 953-977. doi:https://doi.org/10.1016/j.jhydrol.2016.06.006

Kukal, M., & Irmak, S. (2016). Long-term patterns of air temperatures, daily temperature range, precipitation, grass-reference evapotranspiration and aridity index in the USA Great Plains: Part II. Temporal trends. Journal of hydrology, 542, 978-1001.

Kumar, S., Himanshu, S., & Gupta, K. (2012). Effect of global warming on mankind-a review. Int Res J Environ Sci, 1(4), 56-59.

Kunkel, K. E., Andsager, K., & Easterling, D. R. (1999). Long-term trends in extreme precipitation events over the conterminous United States and Canada. Journal of Climate, 12(8), 2515-2527.

Laštuvka, Z. (2009). Climate change and its possible influence on the occurrence and importance of insect pests. Plant Protection Science, 45, S53-S62.

Lipiec, J., Doussan, C., Nosalewicz, A., & Kondracka, K. (2013). Effect of drought and heat stresses on plant growth and yield: a review. International Agrophysics, 27(4), 463-477.

Lobell, D. B., Schlenker, W., & Costa-Roberts, J. (2011). Climate trends and global crop production since 1980. Science, 333(6042), 616-620.

Mallakpour, I., & Villarini, G. (2017). Analysis of changes in the magnitude, frequency, and seasonality of heavy precipitation over the contiguous USA. Theoretical and applied climatology, 130(1), 345-363. doi:10.1007/s00704-016-1881-z

Mann, H. B. (1945). Nonparametric tests against trend. Econometrica: Journal of the econometric society, 245-259.

Martínez, M., Serra, C., Burgueño, A., & Lana, X. (2010). Time trends of daily maximum and minimum temperatures in Catalonia (ne Spain) for the period 1975–2004. International Journal of Climatology: A Journal of the Royal Meteorological Society, 30(2), 267-290.

Masson-Delmotte, V., P. Zhai, A. Pirani, S.L., Connors, C. P., S. Berger, N. Caud, Y. Chen, L. Goldfarb, M.I. Gomis, M. Huang, K. Leitzell, E. Lonnoy, J.B.R., & Matthews, T. K. M., T. Waterfield, O. Yelekçi, R. Yu, and B. Zhou (2021). IPCC, 2021: Climate Change 2021: The Physical Science Basis. Contribution of Working Group I to the Sixth

Assessment Report of the Intergovernmental Panel on Climate Change. Retrieved from

Mastrandrea, M. D., Mach, K. J., Plattner, G.-K., Edenhofer, O., Stocker, T. F., Field, C. B., . . . Matschoss, P. R. (2011). The IPCC AR5 guidance note on consistent treatment of uncertainties: a common approach across the working groups. Climatic Change, 108(4), 675-691.

Menne, M. J., Durre, I., Vose, R. S., Gleason, B. E., & Houston, T. G. (2012). An overview of the global historical climatology network-daily database. Journal of Atmospheric and Oceanic Technology, 29(7), 897-910.

Myhre, G., Alterskjær, K., Stjern, C. W., Hodnebrog, Ø., Marelle, L., Samset, B. H., . . . Schulz, M. (2019). Frequency of extreme precipitation increases extensively with event rareness under global warming. Scientific Reports, 9(1), 1-10.

Nepal, S., & Shrestha, A. B. (2015). Impact of climate change on the hydrological regime of the Indus, Ganges and Brahmaputra river basins: a review of the literature. International Journal of Water Resources Development, 31(2), 201-218.

Nicholls, N. (1997). Increased Australian wheat yield due to recent climate trends. Nature, 387(6632), 484-485.

OWRB. (2012). Oklahoma Water Resources Board- Oklahoma Comprehensive Water Plan: Executive Report, 172 p. Retrieved from

Papalexiou, S. M., & Montanari, A. (2019). Global and regional increase of precipitation extremes under global warming. Water Resources Research, 55(6), 4901-4914.

Patakamuri, S., & Das, B. (2019). Trendchange: innovative trend analysis and time-series change point analysis. The R project for Statistical Computing: Vienna, Austria.

Patakamuri, S., & O'Brien, N. (2021). Modifiedmk: modified versions of Mann Kendall and Spearman's rho trend tests. R package version 1.6. In.

Pathak, P., Kalra, A., & Ahmad, S. (2017). Temperature and precipitation changes in the Midwestern United States: implications for water management. International Journal of Water Resources Development, 33(6), 1003-1019. doi:10.1080/07900627.2016.1238343

Peng, S., Huang, J., Sheehy, J. E., Laza, R. C., Visperas, R. M., Zhong, X., . . . Cassman, K. G. (2004). Rice yields decline with higher night temperature from global warming. Proceedings of the National Academy of Sciences, 101(27), 9971-9975.

Piao, S., Ciais, P., Huang, Y., Shen, Z., Peng, S., Li, J., . . . Fang, J. (2010). The impacts of climate change on water resources and agriculture in China. Nature, 467(7311), 43-51. doi:10.1038/nature09364

Poland, T. M., Patel-Weynand, T., Finch, D. M., Miniat, C. F., Hayes, D. C., & Lopez, V. M. (2021). Invasive Species in Forests and Rangelands of the United States: A Comprehensive Science Synthesis for the United States Forest Sector: Springer Nature.

Seager, R., Lis, N., Feldman, J., Ting, M., Williams, A. P., Nakamura, J., . . . Henderson, N. (2018). Whither the 100th meridian? The once and future physical and human geography of America's arid–humid divide. Part I: The story so far. Earth Interactions, 22(5), 1-22.

Sen, P. K. (1968). Estimates of the regression coefficient based on Kendall's tau. Journal of the American statistical association, 63(324), 1379-1389.

Şen, Z. (2012). Innovative trend analysis methodology. Journal of Hydrologic Engineering, 17(9), 1042-1046.

Şen, Z. (2017). Innovative trend significance test and applications. Theoretical and applied climatology, 127(3-4), 939-947.

Shafer, M., Ojima, D., Antle, J. M., Kluck, D., McPherson, R. A., Petersen, S., . . . Sherman, K. (2014). Ch. 19: great plains. Climate change impacts in the United States: The third national climate assessment, 441-461.

Skendžić, S., Zovko, M., Živković, I. P., Lešić, V., & Lemić, D. (2021). The impact of climate change on agricultural insect pests. Insects, 12(5), 440.

Solomon, S., Qin, D., Manning, M., Chen, Z., Marquis, M., Averyt, K., . . . Miller, H. (2007). IPCC fourth assessment report (AR4). Climate change, 374.

Survey, O. C. (2020). Climate of Oklahoma. Retrieved from https://climate.ok.gov/index.php/site/page/climate_of_oklahoma

Taghvaeian, S., Fox, G., Boman, R., & Warren, J. (2015). Evaluating the impact of drought on surface and groundwater dependent irrigated agriculture in western Oklahoma. Paper presented at the 2015 ASABE/IA Irrigation Symposium: Emerging Technologies for Sustainable Irrigation-A Tribute to the Career of Terry Howell, Sr. Conference Proceedings.

Tao, F., Yokozawa, M., Xu, Y., Hayashi, Y., & Zhang, Z. (2006). Climate changes and trends in phenology and yields of field crops in China, 1981–2000. Agricultural and forest meteorology, 138(1-4), 82-92.

Teegavarapu, R. S. (2012). Floods in a changing climate: extreme precipitation: Cambridge University Press.

Tian, L., & Quiring, S. M. (2019). Spatial and temporal patterns of drought in Oklahoma (1901–2014). International journal of climatology, 39(7), 3365-3378.

Tian, L., & Quiring, S. M. (2019). Spatial and temporal patterns of drought in Oklahoma (1901–2014). International Journal of Climatology, 3365-3378.

Twardosz, R., Walanus, A., & Guzik, I. (2021). Warming in Europe: Recent Trends in Annual and Seasonal temperatures. Pure and Applied Geophysics, 178(10), 4021-4032. doi:10.1007/s00024-021-02860-6

Vose, R. S., Applequist, S., Squires, M., Durre, I., Menne, M. J., Williams Jr, C. N., . . . Arndt, D. (2014). Improved historical temperature and precipitation time series for US climate divisions. Journal of Applied Meteorology and Climatology, 53(5), 1232-1251.

Webb, W. P. (1931). The Great Plains: The University of Nebraska Press.

Willmott, C. J., & Robeson, S. M. (1995). Climatologically aided interpolation (CAI) of terrestrial air temperature. International journal of climatology, 15(2), 221-229.

Zou, Z., Dong, J., Menarguez, M. A., Xiao, X., Qin, Y., Doughty, R. B., . . . Hambright, K. D. (2017). Continued decrease of open surface water body area in Oklahoma during 1984–2015. Science of The Total Environment, 451-460.

Allen. (1996). Assessing integrity of weather data for reference evapotranspiration estimation. Journal of Irrigation and Drainage Engineering, 122(2), 97-106.

Allen, et al. (1983). Weather station siting and consumptive use estimates. Journal of Water Resources Planning and Management, 109(2), 134-136.

Allen, et al. (2011). Evapotranspiration information reporting: II. Recommended documentation. Agricultural Water Management, 98(6), 921-929.

Allen, et al. (1998). Chapter 2-FAO penman-monteith equation. Crop evapotranspiration–Guidelines for computing crop water requirements–FAO Irrigation and drainage paper, 56.

ASAE. (2004). EP505 Measurement and Reporting Practices for Automatic Agricultural Weather Stations.

ASCE. (2005). The ASCE standardized reference evapotranspiration equation. Technical Committee on Standardization of Reference Evapotranspiration.

https://ascelibrary.org/doi/book/10.1061/9780784408056: American Society of Civil Engineers.

ASCE. (2016). Evaporation, evapotranspiration, and irrigation water requirements. Task Committee on Revision of Manual 70: American Society of Civil Engineers.

Baddour, et al. (2007). The role of climatological normals in a changing climate: World Meteorological Organization.

Blankenau, et al. (2020). An evaluation of gridded weather data sets for the purpose of estimating reference evapotranspiration in the United States. Agricultural Water Management, 242, 106376.

Brock, et al. (1995). The Oklahoma Mesonet: a technical overview. Journal of Atmospheric and Oceanic Technology, 12(1), 5-19.

Burman, et al. (1975). Changes in climate and potential evapotranspiration across a large irrigated area in Idaho. Transaction of the ASAE, 18(6), 1089-1093.

Cai, et al. (2007). Estimating reference evapotranspiration with the FAO Penman–Monteith equation using daily weather forecast messages. Agricultural and Forest Meteorology, 145(1-2), 22-35.

Daly, et al. (1994). A statistical-topographic model for mapping climatological precipitation over mountainous terrain. Journal of Applied Meteorology and Climatology, 33(2), 140-158.

Davenport, et al. (1967). Meteorological observations and Penman estimates along a 17-km transect in the Sudan Gezira. Agricultural Meteorology, 4(6), 405-414.

De Vries, et al. (1961). The modification of climate near the ground by irrigation for pastures on the Riverine Plain. Australian Journal of Agricultural Research, 12(2), 260-272.

Fiebrich, et al. (2001). The impact of unique meteorological phenomena detected by the Oklahoma Mesonet and ARS Micronet on automated quality control. Bulletin of the American Meteorological Society, 82(10), 2173-2188.

Fiebrich, et al. (2010). Quality Assurance Procedures for Mesoscale Meteorological Data. Journal of Atmospheric and Oceanic Technology, 27(10), 1565-1582. doi:10.1175/2010jtecha1433.1

Itenfisu, et al. (2002). Spatial and temporal variability in reference evapotranspiration in Oklahoma. Energy, climate, environment and water-issues and opportunities for irrigation and drainage, San Luis Obispo, California, July 9-12, 2002.

Jia, et al. (2004). Temperature adjustment for reference evapotranspiration calculation in Central Arizona. Journal of Irrigation and Drainage Engineering, 130(5), 384-390.

Ley, et al. (1994). Energy and soil water balance analyses of arid weather sites. Paper presented at the Proc. ASAE Int. Summer Meeting, American Society of Agricultural Engineers, St. Joseph, Mich.

McPherson, et al. (2007). Statewide monitoring of the mesoscale environment: A technical update on the Oklahoma Mesonet. Journal of Atmospheric and Oceanic Technology, 24(3), 301-321.

Myers, et al. (2010). Research design and statistical analysis: Routledge.

Richard G. Allen. (2016). Ref-ET Software. Evapotranspiration Calculator Users Manual Ver 4.1 (Version 4.1): Kimberly Research and Extension Center, University of Idaho. Retrieved from www.uidaho.edu/cals/kimberly-research-and-extension-center/research/water-resources/ref-et-software

Seager, et al. (2018). Whither the 100th meridian? The once and future physical and human geography of America's arid–humid divide. Part I: The story so far. Earth Interactions, 22(5), 1-22.

Shafer, et al. (1993). The Oklahoma mesonet: Site selection and layout. Paper presented at the Preprints, Eighth Symp. on Meteorological Observations and Instrumentation, Anaheim, CA, Amer. Meteor. Soc.

Spearman. (1961). The proof and measurement of association between two things.

Svoboda, et al. (2002). The drought monitor. Bulletin of the American Meteorological Society, 83(8), 1181-1190.

Temesgen, et al. (1999). Adjusting temperature parameters to reflect well-watered conditions. Journal of Irrigation and Drainage Engineering, 125(1), 26-33.

Vanella, et al. (2020). Comparing the use of past and forecast weather data for estimating reference evapotranspiration. Agricultural and Forest Meteorology, 295, 108196.

Webb. (1931). The Great Plains: The University of Nebraska Press.

WMO. (2018). Guide to Instruments and Methods of Observation. In: World Meteorological Organization Geneva.

Allen, R. G. (1996). Assessing integrity of weather data for reference evapotranspiration estimation. Journal of irrigation and drainage engineering, 122(2), 97-106.

Allen, R. G. (2006). Footprint analysis to assess the conditioning of temperature and humidity measurements in a weather station vicinity. World Environmental and Water Resource Congress 2006: Examining the Confluence of Environmental and Water Concerns,

ASCE-EWRI. (2005). The ASCE standardized reference evapotranspiration equation. In (pp. 213): American Society of Civil Engineers (ASCE) Reston, VA.

ASCE. (2005). The ASCE standardized reference evapotranspiration equation. Technical Committee on Standardization of Reference Evapotranspiration.

https://ascelibrary.org/doi/book/10.1061/9780784408056. American Society of Civil Engineers.

Blankenau, P. A., Kilic, A., & Allen, R. (2020). An evaluation of gridded weather data sets for the purpose of estimating reference evapotranspiration in the United States. Agricultural Water Management, 242, 106376.

Esquerdo, J., Zullo Júnior, J., & Antunes, J. (2011). Use of NDVI/AVHRR time-series profiles for soybean crop monitoring in Brazil. International Journal of Remote Sensing, 32(13), 3711-3727.

Fiebrich, C. A., Morgan, C. R., McCombs, A. G., Hall, P. K., & McPherson, R. A. (2010). Quality assurance procedures for mesoscale meteorological data. Journal of Atmospheric and Oceanic Technology, 27(10), 1565-1582.

Gash, J. H. C. (1986). A note on estimating the effect of a limited fetch on micrometeorological evaporation measurements. Boundary-Layer Meteorology, 35(4), 409-413. https://doi.org/10.1007/BF00118567

Huntington, J., McGwire, K., Morton, C., Snyder, K., Peterson, S., Erickson, T., Niswonger, R., Carroll, R., Smith, G., & Allen, R. (2016). Assessing the role of climate and resource management on groundwater dependent ecosystem changes in arid environments with the Landsat archive. Remote sensing of Environment, 185, 186-197.

Jensen, D., Hargreaves, G., Temesgen, B., & Allen, R. (1997). Computation of ETo under nonideal conditions. Journal of irrigation and drainage engineering, 123(5), 394-400.

Jensen, M., & Allen, R. (2016). Evaporation, evapotranspiration, and irrigation water requirements: Task Committee on Revision of Manual 70. Evaporation, evapotranspiration, and irrigation water requirements: Task Committee on Revision of Manual 70.(Ed. 2).

Ji-Hua, M., & Bing-Fang, W. (2008). Study on the crop condition monitoring methods with remote sensing. International Archives of the Photogrammetry, Remote Sensing and Spatial Information Sciences, 37(B8), 945-950.

Jia, X., Dukes, M. D., Jacobs, J. M., & Haley, M. (2007). Impact of weather station fetch distance on reference evapotranspiration calculation. World Environmental and Water Resources Congress 2007: Restoring Our Natural Habitat,

Jia, X., Martin, E., & Slack, D. (2004). Temperature adjustment for reference evapotranspiration calculation in Central Arizona. Journal of irrigation and drainage engineering, 130(5), 384-390.

Kljun, N., Kastner-Klein, P., Fedorovich, E., & Rotach, M. (2004). Evaluation of Lagrangian footprint model using data from wind tunnel convective boundary layer. Agricultural and forest meteorology, 127(3-4), 189-201.

Leclerc, M. Y., Shen, S., & Lamb, B. (1997). Observations and large-eddy simulation modeling of footprints in the lower convective boundary layer. Journal of Geophysical Research: Atmospheres, 102(D8), 9323-9334.

Llasat, M., & Snyder, R. (1998). Data error effects on net radiation and evapotranspiration estimation. Agricultural and forest meteorology, 91(3-4), 209-221.

Rangoonwala, A., Ahmed, S., Nasir, A., Raouf, A., & Shahab, H. (1993). Quasi-operational use of NOAA/AVHRR vegetation index to monitor vegetal cover and crop growth. Advances in Space Research, 13(5), 265-268.

Schmid, H. P. (2002). Footprint modeling for vegetation atmosphere exchange studies: a review and perspective. Agricultural and forest meteorology, 113(1-4), 159-183.

Schuepp, P., Leclerc, M., MacPherson, J., & Desjardins, R. (1990). Footprint prediction of scalar fluxes from analytical solutions of the diffusion equation. Boundary-Layer Meteorology, 50(1), 355-373.

Shafer, M. A., Fiebrich, C. A., Arndt, D. S., Fredrickson, S. E., & Hughes, T. W. (2000). Quality assurance procedures in the Oklahoma Mesonetwork. Journal of Atmospheric and Oceanic Technology, 17(4), 474-494.

Temesgen, B., Allen, R., & Jensen, D. (1999). Adjusting temperature parameters to reflect well-watered conditions. Journal of irrigation and drainage engineering, 125(1), 26-33.

Trajkovic, S., & Kolakovic, S. (2009). Estimating reference evapotranspiration using limited weather data. Journal of irrigation and drainage engineering, 135(4), 443-449.

Wilhite, D. A. (2000). Drought as a natural hazard: concepts and definitions.

Yang, Z., Di, L., Yu, G., & Chen, Z. (2011). Vegetation condition indices for crop vegetation condition monitoring. 2011 IEEE International Geoscience and Remote Sensing Symposium,

Yoder, R. E., Ley, T. W., & Elliott, R. L. (2000). Measurement and reporting practices for automatic agricultural weather stations.

Zhang, M., Wu, B., Yu, M., Zou, W., & Zheng, Y. (2014). Crop condition assessment with adjusted NDVI using the uncropped arable land ratio. Remote sensing, 6(6), 5774-5794.

APPENDICES

This Supplementary Material file includes 5 figures.

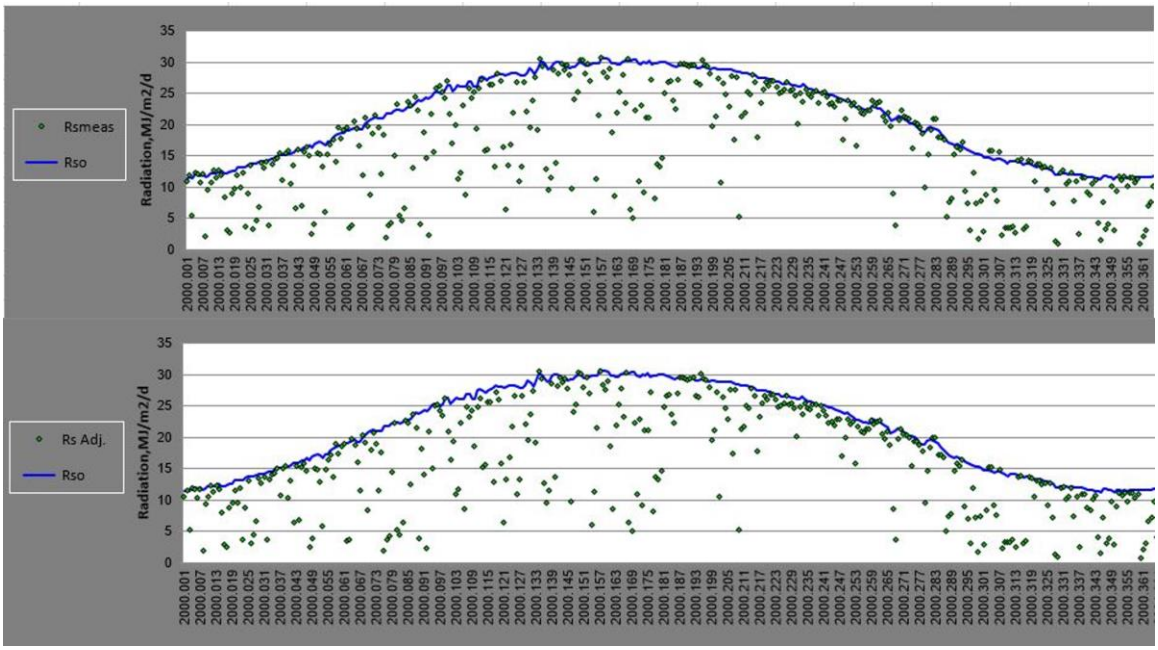

Fig. S1- Measured (Rs) and adjusted (Rs,adj) solar radiation against the theoretical clear sky solar radiation (Rso) for Stillwater (STIL) station.

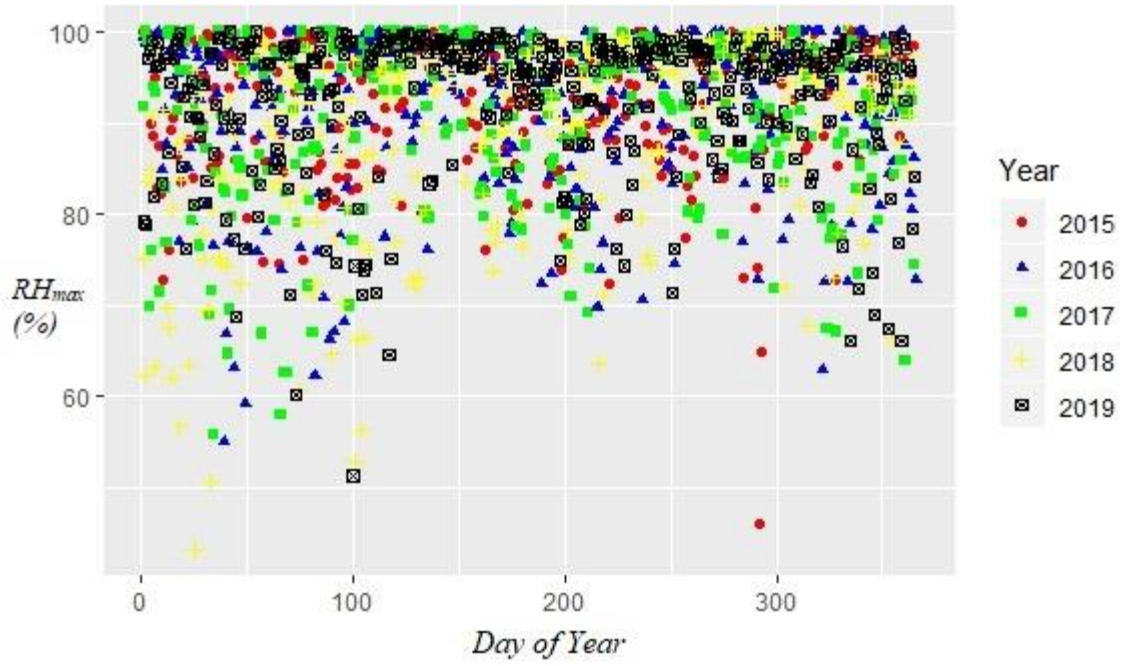

Fig. S2. Daily values of RHmax at Stillwater Mesonet station (2015 -2019) showing proper sensor calibration and measurements

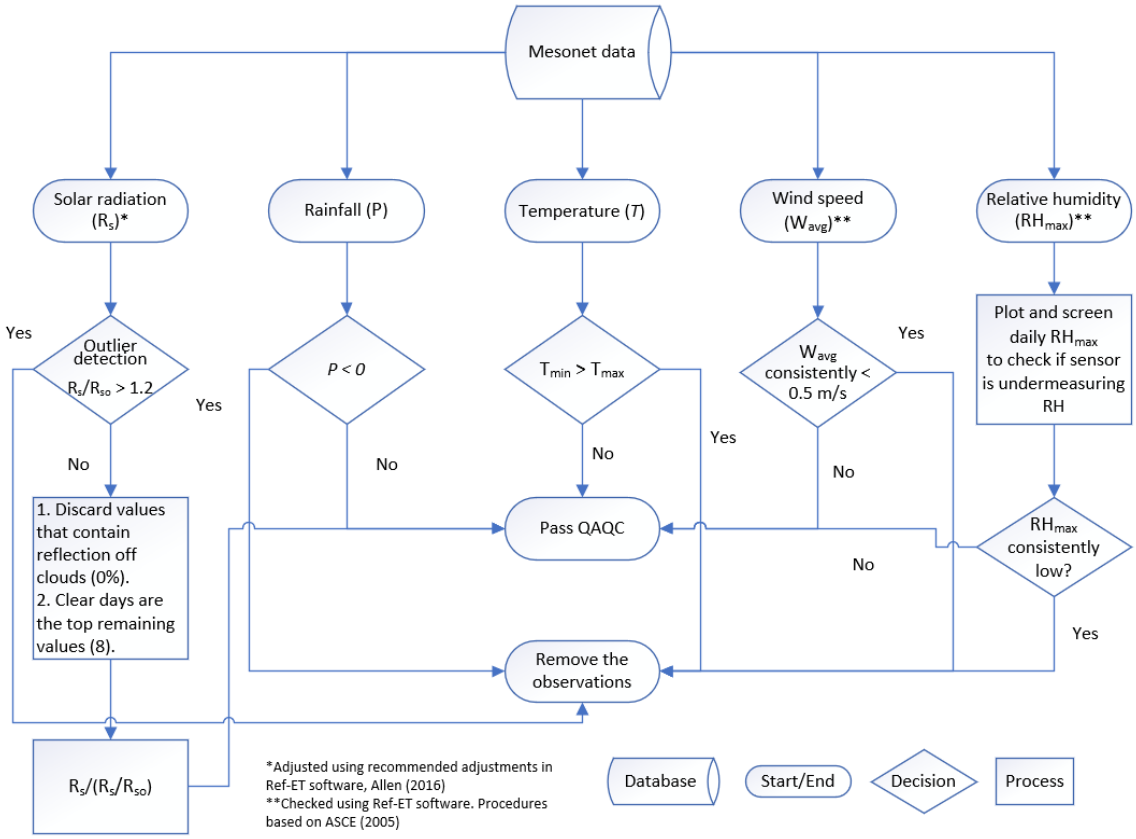

Fig. S3. Flowchart of the quality assurance and quality control (QAQC) steps implemented in the study in addition to the Mesonet's standard QAQC procedure.

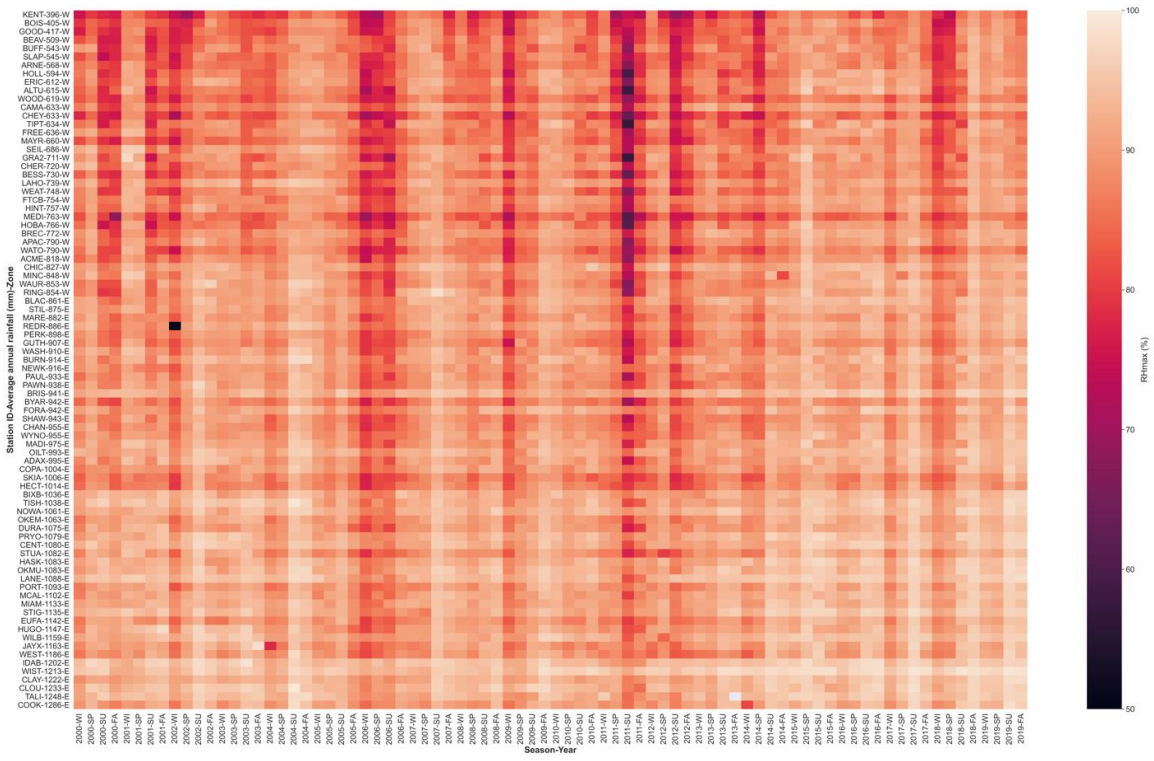

Fig. S4. Spatiotemporal variation of seasonal RHmax in western (W) and eastern (E) stations sorted ascendingly based on rainfall.

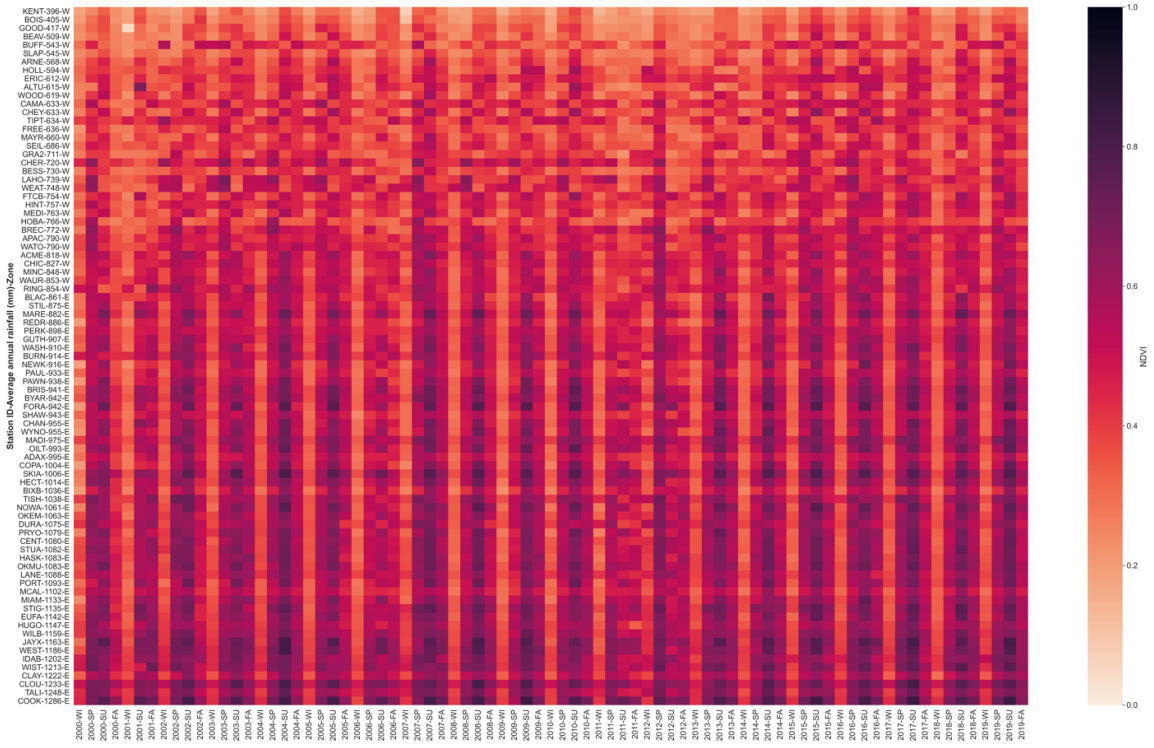

Fig S5. Spatiotemporal variation of seasonal NDVI in western (W) and eastern (E) stations sorted ascendingly based on rainfall.

VITA

Aseem Pal Singh

Candidate for the Degree of

Doctor of Philosophy

Dissertation: CHARACTERIZING STATION ARIDITY AND IMPROVING THE ESTIMATES OF REFERENCE EVAPOTRANSPIRATION IN THE OKLAHOMA MESONET

Major Field: Biosystems Engineering

Biographical:

Education:

Completed the requirements for the Doctor of Philosophy in Biosystems Engineering at Oklahoma State University, Stillwater, Oklahoma in July, 2022.

Completed the requirements for the Master of Technology in Environmental Management at Indian Institute of Technology, Roorkee, India in 2015.

Completed the requirements for the Bachelor of Technology in Civil Engineering at G.B. Pant University of Agriculture and Technology, Pantnagar, India in 2012.

Experience:

Graduate Research Assistant	2019-2022
Oklahoma State University, Stillwater, Oklahoma	
Graduate Teaching Assistant	2020-2021
Oklahoma State University, Stillwater, Oklahoma	
Assistant Engineer	2017-2018
Irrigation Department, Uttarakhand, India	

Professional Memberships:

American Geophysical Union	2019
American Society of Civil Engineers	2020-present
American Society of Agricultural and Biological Engineers	2019-present